

What we learn from mushrooms: natural history data as a resource in fungal ecology

A DISSERTATION

SUBMITTED TO THE FACULTY OF THE
UNIVERSITY OF MINNESOTA

BY

Talia Joan Michaud

IN PARTIAL FULFILLMENT OF THE REQUIREMENTS

FOR THE DEGREE OF
DOCTOR OF PHILOSOPHY

Dr. Peter G. Kennedy

May 2024

Acknowledgements

I am endlessly grateful for my family and friends for supporting me through this challenging series of projects. Their unconditional support makes me feel like I can take on the world, or write a thesis in fungal ecology. Thanks in no particular order to Lang, for letting me talk nonsense on canoes, Olive, for feeding me so much chickpea curry and other nourishment, Aaron, for being snarky with me and enjoying plants, Nishia for our decompression coffee runs, Anahi and Achala for being so darn kind, Katie for always bringing a smile to my face, and Eduardo for those long isotope chats of old. Thanks to Sabra for letting me spend time with the parrots and talk about life. Thanks to my parents. When I say unconditionally supportive, that's what I mean.

Thanks to my collaborators, especially Erik Hobbie for his stable isotope truthing, Ian Pearse for his wealth of masting knowledge and kindness, and Håvard Kauserud for his encouragement and generosity. Thanks to other members of my committee: Sarah Hobbie, Daniel Stanton, and Jonathan Schilling for their careful comments and support. I am grateful for my funding sources, beginning with the College of Biological Sciences Dean's Distinguished Graduate Fellowship in my first year. Thanks to the Minnesota Mycological Society for two awards, and to the Bell Museum of Natural History for the Joyce Davenport Fellowship. Thanks to the Norwegian Centennial Chair Program for the award enabling me to meet my collaborator Håvard Kauserud in Oslo. Finally, this work was in part supported by several NSF grants, including an NSF RUBC Postdoctoral Fellowship to Lauren Cline, and two NSF grants to Peter Kennedy.

Dedication

This work is dedicated to my family, *sensu lato*

Table of Contents

Acknowledgements.....	i
Dedication.....	ii
Table of Contents.....	iii
List of Tables.....	iv
List of Figures.....	v
Introduction.....	1
Chapter 1: Herbarium specimens reveal that mycorrhizal type does not mediate declining temperate tree nitrogen status over more than a century of environmental change.....	5
Chapter 2: Carbon cycling through plant and fungal herbarium specimens tracks the Suess effect over more than a century of environmental change.....	28
Chapter 3: Mast seeding in European beech (<i>Fagus sylvatica</i> L.) is associated with reduced fungal sporocarp production and community diversity.....	46
Bibliography.....	73
Appendices.....	84

List of Tables

Table 1.1. Summary of fixed effects in mixed model of ectomycorrhizal and arbuscular mycorrhizal foliar $\delta^{15}\text{N}$ across the United States.

Table 2.1. Genus-level summary of collections analyzed in this study.

Table 3.1. Descriptions of 25 most abundant fungal species observed at La Chanéaz, with reference to their association with European beech seed production.

List of Figures

Figure 1.1. Summary of foliar and sporocarp samples from herbarium collections made in Minnesota, USA, from 1871 to 2016.

Figure 1.2. Summary of foliar data from arbuscular mycorrhizal and ectomycorrhizal plants analyzed across the United States with reference to contemporaneous atmospheric carbon dioxide levels and nitrogen deposition.

Figure 1.3. Temporal trends in measured and modeled [N] and $\delta^{15}\text{N}$ among ectomycorrhizal plants, arbuscular mycorrhizal plants, ectomycorrhizal fungi, and saprotrophic fungi in Minnesota, USA, from 1871 to 2016.

Figure 1.4. Changes in ^{15}N depletion in ectomycorrhizal versus arbuscular mycorrhizal leaves across 145 years in Minnesota, USA and relative to atmospheric nitrogen deposition rates across the United States.

Figure 2.1. Trends in tissue $\delta^{13}\text{C}$ among herbarium specimens over time.

Figure 2.2. Breakpoint estimates in $\delta^{13}\text{C}$ over 14 decades among plants, fungi, and the atmosphere.

Figure 2.3. Patterns in the $\delta^{13}\text{C}$ decline over time of twig-rotting and log-rotting saprotrophic fungi.

Figure 3.1. Climate (panels one and two) and beech seed production (third panel) data from 1977–2006 for Payerne, Switzerland.

Figure 3.2. Relationship between European beech seed production and sporocarp production from 1977–2006.

Figure 3.3. Distance-based redundancy analysis showing the relationships between fungal sporocarp community composition, climate, and European beech seed production.

Figure 3.4. Variation in fungal species' relationships with European beech seed production derived from multiple logistic regression models.

Introduction

Through their diverse ecological roles as mutualists, saprotrophs, and pathogens, fungi play a fundamental role in mediating forest carbon capture. Understanding fungal responses to global environmental change is therefore central to predicting forest feedbacks to accumulating atmospheric carbon dioxide. Short term research that isolates drivers of environmental change are common, despite knowledge that drivers of environmental change interact, producing emergent effects at multidecadal timescales. Similarly, existing research typically isolates fungal responses, though fungal activity is contingent on the activity of other organisms, particularly plants. In this context, I sought to produce research in my doctoral thesis that integrated plant and fungal responses to environmental change using natural history data. The use of herbarium collections and field surveys of fungal sporocarps (mushrooms) enables analysis spanning multiple decades, which can capture the cumulative effects of multiple drivers of environmental change. Together, my thesis hinges on documentation of fungi and plants in their natural environment, often called natural history data, and highlights the promising potential for using this approach in global change research.

My first chapter reconstructs plant and fungal responses to 145 years of environmental change in Minnesota, USA, using herbarium specimens. Over this timespan, Minnesota has experienced variation in two key drivers of environmental change, namely six-fold variation in atmospheric nitrogen deposition, and a 40% increase in atmospheric carbon dioxide concentrations. These drivers are posited to have contrasting effects on plant

associating with different mycorrhizal fungal types. Specifically, ectomycorrhizal fungi capable of organic nitrogen capture are thought to enhance plant nitrogen status under rising carbon dioxide concentrations, sustaining fertilized growth. Arbuscular mycorrhizal fungi, on the other hand, are thought to advantage their hosts under atmospheric nitrogen deposition that increases inorganic nitrogen availability, which they are specialized in acquiring. Meanwhile, ectomycorrhizal fungi are variably sensitive to nitrogen deposition, which has been shown to select for a subset of the ectomycorrhizal fungal community. The combined effects of long-term atmospheric nitrogen deposition and atmospheric carbon dioxide accumulation on plant and fungal nitrogen status were unknown, however. This chapter revealed that mycorrhizal type did not mediate plant nitrogen status. Instead, plant and ectomycorrhizal fungal nitrogen concentrations declined over time, despite nitrogen deposition. Additionally, by conducting an analysis of spatially distributed foliar $\delta^{15}\text{N}$ data that had been previously published, I found evidence that nitrogen deposition was associated with changing ectomycorrhizal nitrogen dynamics. These findings highlight the use of natural history data in validating results from short-term experiments.

My second chapter similarly reconstructs aspects of carbon cycling over the same timescale in Minnesota, USA. Specifically, I tested whether herbarium specimens could be used to track variation in the isotopic composition of atmospheric carbon dioxide known as the Suess effect. The Suess effect is characterized by a non-linear decline in atmospheric $\delta^{13}\text{C}$, or the ratio of heavy ^{13}C to light ^{12}C . This decline is driven by the combustion of fossil fuels, which is ^{13}C -depleted and effectively labels atmospheric carbon dioxide. By

combining data from plant and fungal collections, I found evidence that plants and ectomycorrhizal fungi build leaves and sporocarps with recently fixed carbon, while sporocarps of saprotrophic fungi, on average, were constructed with carbon fixed 32–55 years ago. I also found that $\delta^{13}\text{C}$ trends depended on the age of saprotrophic fungal carbon, with those growing on twigs more closely tracking atmospheric $\delta^{13}\text{C}$ than those growing on logs. These results demonstrated that plant and fungal collections were sensitive to the Suess effect. I proposed that this finding may have applications in future research, for instance in assessing carbon sources among different taxa of forest fungi.

My final chapter assesses the effects of mast seeding, an endemic source of environmental change, on fungal activity and community composition. Mast seeding is a widespread environmental phenomenon characterized by high interannual variability in seed production among perennial plants. Years with outsized seed production are referred to as mast years. Trees often switch resources away from vegetative growth to produce a mast seed crop. Limited evidence suggests this resource switching extends belowground, with decreased fine root production observed in a mast year. Whether resource switching effects forest fungi was previously unknown: the intersection of masting and fungal ecology represents a novel line of research. To reconstruct the relationship between interannual variability in seed production and fungal resource availability and sporocarp production, I combined two sources of natural history data: a fungal census spanning 29 years from near Payerne, Switzerland, and a time series of seed production data from the dominant overstory tree species, European beech (*Fagus sylvatica*). Findings suggested that seed

production and fungal sporocarp production are tightly linked. Sporocarp production declined 55% in the year with the highest recorded seed production. Furthermore, sporocarp community composition was significantly related to seed production, while community diversity and species richness declined with increasing seed production. Together, these results are consistent with the hypothesis that resource switching during a mast year has belowground consequences, limiting fungal reproductive investment. Mast seeding, therefore, may be an underappreciated driver of fungal activity.

Predicting ecosystem responses to environmental change is urgently needed. Natural history collections have the potential to aid us by showing how ecosystems have responded to change that has already occurred. My thesis is united by several themes, including multidecadal timescales and coupled plant and fungal datasets, enabled by natural history data. My first chapter highlights that cumulative effects of long-term environmental change can defy expectations from short-term experiments. My second chapter reveals a novel use for herbarium specimens for tracking ecosystem carbon cycling. Finally, my third chapter suggests an underappreciated driver of fungal resource availability, mast seeding. Together, this work highlights the utility of natural history data in looking backwards to better anticipate the future.

Chapter 1

Herbarium specimens reveal that mycorrhizal type does not mediate declining temperate tree nitrogen status over more than a century of environmental change

Summary

Rising atmospheric carbon dioxide concentrations (CO₂) and atmospheric nitrogen (N) deposition have contrasting effects on ectomycorrhizal (EM) and arbuscular mycorrhizal (AM) symbioses, potentially mediating forest responses to environmental change. In this study, we evaluated the cumulative effects of historical environmental change on N concentrations and $\delta^{15}\text{N}$ values in AM plants, EM plants, EM fungi, and saprotrophic fungi using herbarium specimens collected in Minnesota, USA from 1871 to 2016. To better understand mycorrhizal mediation of foliar $\delta^{15}\text{N}$, we also analyzed a subset of previously published foliar $\delta^{15}\text{N}$ values from across the United States to parse the effects of N deposition and CO₂ rise. Over the last century in Minnesota, N concentrations declined among all groups except saprotrophic fungi. $\delta^{15}\text{N}$ also declined among all groups of plants and fungi; however, foliar $\delta^{15}\text{N}$ declined less in EM plants than in AM plants. In the analysis of previously published foliar $\delta^{15}\text{N}$ values, this slope difference between EM and AM plants was better explained by nitrogen deposition than by CO₂ rise. Mycorrhizal type did not explain trajectories of plant N concentrations. Instead, plants and EM fungi exhibited similar declines in N concentrations, consistent with declining forest N status despite moderate levels of N deposition.

Introduction

Mycorrhizal type is increasingly invoked to predict forest responses to environmental change (Terrer et al., 2016; Averill et al., 2018; Baldrian et al., 2023). Most trees associate with either ectomycorrhizal (EM) or arbuscular mycorrhizal (AM) fungi (Steidinger et al., 2019), which differ in their nutrient acquisition strategies (Smith & Read, 2010). Because EM fungi can obtain nutrients directly from organic matter (Frey, 2019; Lindahl & Tunlid, 2015; Shah et al., 2016), EM plants are better adapted to conditions of low inorganic nutrient availability, while AM plants and fungi are better adapted to inorganic nutrient acquisition (Phillips et al., 2013). As such, mycorrhizal type may mediate forest responses to environmental changes that alter soil nutrient availability or demand, such as atmospheric nitrogen (N) deposition or rising carbon dioxide (CO₂) concentrations (Mohan et al., 2014).

Atmospheric N deposition increases inputs of bioavailable inorganic N to soils (Galloway et al., 2004). Consistent with the idea that AM symbionts are better adapted to soils with high inorganic nutrient availability, Averill et al. (2018) found that AM tree recruitment increased and EM tree recruitment decreased with greater amounts of N deposition across the United States. Concurrently, some EM fungi appear sensitive to N deposition, evidenced by marked declines in sporocarp production followed by a shift in belowground community structure towards “nitrotolerant” species (Arnolds, 1991; Lilleskov et al., 2011). Indicators of decreased belowground EM fungal abundance have been documented

with N addition (P. Högberg et al., 2011), although this potential consequence is often overgeneralized (Karst et al., 2021; Lilleskov et al., 2019).

Rising atmospheric CO₂, however, may favor EM plants and fungi if increasing CO₂ concentrations stimulate plant N demand, requiring increased N acquisition from organic pools (Pellitier et al., 2021). Historical declines in plant tissue $\delta^{15}\text{N}$ and [N] have been interpreted as evidence that rising CO₂ stimulates plant N demand, decreasing ecosystem N-loss pathways that discriminate against ¹⁵N (McLauchlan et al., 2010; Craine et al., 2018;). Further, in a meta-analysis of free air CO₂ enrichment studies, elevated CO₂ enhanced growth of EM plants but not AM plants at low N availability sites (Terrer et al., 2016). Alternatively, in highly N-limited environments, such as boreal forests (Näsholm et al., 2013), EM fungi may instead limit N availability to plants under rising CO₂ by outcompeting plants for N (Alberton et al., 2007; Dong et al., 2018).

The analysis of herbarium collections offers a novel opportunity to evaluate the effects of rising atmospheric CO₂ and N deposition on plant N status over historical increases in both global change drivers. For instance, historical declines in foliar N concentrations and $\delta^{15}\text{N}$ reported across terrestrial ecosystems (Craine et al., 2018) may not occur in an area with historical N deposition, particularly among AM plants better adapted to acquire inorganic N. In contrast, increased plant N demand under rising CO₂ may swamp N inputs from N deposition, resulting in declining foliar N concentrations and $\delta^{15}\text{N}$. However, these declines may be smaller or nonexistent among EM plants if their N supply can be

supplemented by organic N. Alternatively, if N deposition mitigates organic N access among EM fungi and by extension, their ability to supplement plant N, while failing to directly satisfy increasing plant N demand, EM and AM plants may show similar declines in N concentrations under rising CO₂.

Since fungi are both subject to and mediators of soil N availability, sampling fungal herbarium collections in addition to plants allows for assessment of whether fungi have experienced concomitant declines in indices of fungal N status (Hobbie et al., 2019; Kranabetter et al., 2019) that have been observed in plant tissues (Craine et al., 2018). The long-term trajectories of fungal N status may, however, differ by ecological guild (saprotrophic versus EM). For example, EM fungi with ready access to photosynthate may outcompete saprotrophic fungi for soil N (Fernandez et al., 2019), potentially stabilizing N acquisition over environmental changes.

To evaluate the cumulative effects of historical environmental change on plant and fungal N status, we analyzed N concentrations and $\delta^{15}\text{N}$ among 493 plant and fungal collections made in Minnesota from 1871 – 2016. Over this period, atmospheric N deposition varied six-fold in Minnesota, peaking at 18 kg ha⁻¹ year⁻¹ in the 1990s (Clark et al., 2018) and atmospheric CO₂ increased by 40% (Belmecheri & Lavergne, 2020). This region was therefore well-suited for evaluating the cumulative effects of historical N deposition and CO₂ increase. Specifically, we tested whether 1) plant and fungal N concentrations and $\delta^{15}\text{N}$ declined in an area experiencing CO₂ rise and increasing N deposition and 2)

trajectories of plant $\delta^{15}\text{N}$ and N concentrations diverged by mycorrhizal type. We also analyzed a subset of previously published foliar $\delta^{15}\text{N}$ values (Craine et al., 2019) to parse the effects of CO_2 rise, N deposition, and mycorrhizal controls of $\delta^{15}\text{N}$. In this second dataset, we tested the extent to which 1) CO_2 rise or N deposition explain declines in foliar $\delta^{15}\text{N}$ and 2) $\delta^{15}\text{N}$ trajectories diverged by mycorrhizal type with CO_2 rise or N deposition.

Materials and Methods

Herbarium study: sample selection

324 plant and 232 fungal specimens were selected from the collections at the Bell Herbarium at the University of Minnesota from within a 130 km radius surrounding the University of Minnesota Saint Paul Campus, USA (44.9849° N, 93.1853° W) (Figure 1.1, Figure 1.2a). This area is composed of temperate hardwood forests, with a mean annual temperature of 7.2 °C and annual precipitation of approximately 838 mm. Samples were selected from genera whose records spanned at least 8 decades between 1880 and 2010. The 16 genera sampled belong to four ecological groups: EM plants, AM plants, EM fungi, and saprotrophic fungi (AM fungi do not typically produce macroscopic sporocarps, so could not be included). To eliminate effects of plant life form, we selected only broadleaf deciduous genera. Plant mycorrhizal type was assigned using the FungalRoot database (Soudzilovskaia et al., 2019). Because herbarium collections were made from mature *Populus* individuals, we considered *Populus* EM-associated (Teste et al., 2020).

Fungal taxonomy was manually updated to reflect current knowledge; some collections, however, lacked species-level identification ($n = 16$). Out of 55 species represented in the collections, the median number of samples per species was two. Because we were interested in accounting for species-level variation, we excluded samples without species identity and from species with fewer than three representatives ($n_{\text{removed}} = 63$, $n_{\text{fungi retained}} = 169$, $n_{\text{all retained}} = 493$). The EM fungal genus *Tricholoma* was excluded after this step because of sparse species-level collections. Summary information about the final dataset are in Appendix S1.3 and Figure 1.1.

Herbarium study: elemental and isotopic analysis

Foliar and sporocarp tissues were homogenized prior to analysis via either an Elementar Vario Pyrocube (Hanau, Germany) interfaced to an Isoprime 100 isotope ratio mass spectrometer (Cheadle, UK) at the University of Minnesota or an Elementar Vario EL Cube interfaced to a PDZ Europa 20-20 isotope ratio mass spectrometer (Sercon Ltd., Cheshire, UK) at the University of California-Davis Stable Isotope Facility. See Appendices S1.1 and S1.2 for quality control steps to ensure consistent data between the two facilities.

Herbarium study: statistical analyses

All statistical analyses were performed in R, version 4.3.0 (R Core Team, 2023). Models were fitted using the lmer function in the lme4 package (Bates et al., 2015), p-values produced using Satterthwaite's approximations of degrees of freedom with the lmerTest

package (Kuznetsova et al., 2017). Prediction intervals were produced using the `predictInterval` function in the `merTools` package (Knowles & Frederick, 2016).

Initial models included random effects to account for potential effects of species identity, genus, seasonality (month), and geographic location (county). To evaluate potential differences in baseline [N] and $\delta^{15}\text{N}$ and temporal trends between groups, the fixed effects of year, group, and their interaction were included. Year was a continuous variable (0-145 corresponding to years 1871-2016) and group was a categorical variable (EM plant, AM plant, EM fungus, saprotrophic fungus). Backwards stepwise selection using the function `step` in the `lmerTest` package (Kuznetsova et al., 2017) was performed on the random effects to improve model parsimony and avoid overfitting. Final models included only the preserved random effects and original fixed effects.

Models of foliar and sporocarp [N] were run separately on plants and fungi, given differences between leaf and mushroom stoichiometry. Natural log-transformed [N] values were used to satisfy the assumption of heteroscedasticity. Back-transformed statistics are reported in the text to aid interpretation. In the model of foliar [N], preserved random effects accounted for differences in seasonality (month), geography (county), and species and genus identity (species nested within genus). Backwards stepwise selection on the model of sporocarp [N] eliminated the effects of seasonality, preserving species nested within genus and county.

Sporocarp and foliar $\delta^{15}\text{N}$ were modeled globally, treating $\delta^{15}\text{N}$ as a tracer comparable across leaves and mushrooms. Comparing trajectories of foliar $\delta^{15}\text{N}$ between EM and AM plants allows us to test potential mycorrhizal controls of $\delta^{15}\text{N}$. Specifically, the leaves of EM plants are typically ^{15}N -depleted relative to AM leaves, reflecting the preferential transfer of ^{15}N -depleted N compounds from EM fungi to their plant partners (Craine et al., 2009). ^{15}N depletion of transfer compounds is driven by both the fractionation that occurs during compound synthesis, and preferential retention of ^{15}N in EM fungal biomass (Hobbie & Högberg, 2012). EM foliar N may thus become less ^{15}N -depleted relative to AM foliar N when 1) EM plants source less N from EM fungi overall or 2) less ^{15}N is retained in EM fungal biomass (Hobbie & Colpaert, 2003). As in the [N] models, the full set of possible random effects was reduced using backwards stepwise selection. The final set of random effects included species identity nested within genus. Fixed effects, as in the [N] model, included group, year, and their interaction to test for different temporal trends across groups.

Spatial foliar $\delta^{15}\text{N}$ analysis: data compilation

We extracted foliar $\delta^{15}\text{N}$ and [N] data from Craine et al. (2018) (Craine et al., 2019), in which each $\delta^{15}\text{N}$ and [N] value represents an average for a given species at a given site (defined by 0.1° latitude/longitude or ~ 11 km) in one year. We subsampled this data to only include EM and AM plants in the USA ($n = 2138$: $n_{\text{EM}} = 845$, $n_{\text{AM}} = 1293$, $n_{\text{species}} = 299$). While we were initially only interested in trees, data from AM trees were far less abundant than EM trees, resulting in an imbalanced dataset. We therefore included

herbaceous plants as well, adding in random effects based on taxonomy in our model structure to account for the effects of life form, and excluded plants from AM-only ecosystems (explained later). These data cover the period from 1980 to 2016. The original publication contains full details about data collection, mycorrhizal type assignment, and quality control procedures (Craine et al., 2018).

We next compiled additional features at the same geographic scale that might capture variation in foliar $\delta^{15}\text{N}$, including climatic variables (mean annual temperature, aridity index, mean annual precipitation, net primary productivity), edaphic features (soil pH, organic C content, total N, cation exchange capacity, clay, silt, sand fractions, and bulk density topsoil), land cover features (developed/cultivated land), and vegetation features (woody/herbaceous cover, EM/AM root stocks). We also included the 182 level III ecoregions of North America (Bailey, 2014) to capture potential emergent effects of ecoregion. Annual atmospheric CO_2 concentrations were compiled from Belmecheri & Lavergne (2020). Gridded decadal estimates of annual N deposition at 12 x 12 km resolution were extracted for each site from Clark et al. (2018). Projected EM/AM root stocks (Mg C ha^{-1}) were extracted from Barceló et al. (2023) as a proxy for potential EM/AM fungal abundance. The proportion of the colonized mycorrhizal root stock belonging to EM plants was calculated for statistical analyses to represent EM fungal “dominance.” Due to our interest in modelling EM $\delta^{15}\text{N}$ relative to AM $\delta^{15}\text{N}$ from comparable ecosystems, we excluded all sites with estimated EM root stocks at 0 Mg C ha^{-1} ($n = 782$).

All data layers were aggregated to 10 km x 10 km to approximate the resolution of the averaged foliar $\delta^{15}\text{N}$ and [N] values from Craine et al. (2018). After combining all data layers and excluding missing values, the final dataset contained 1108 observations ($n_{\text{EM}} = 466$, $n_{\text{AM}} = 639$). Information about the frequency of species/genera included in the final dataset and their mycorrhizal type is presented in Appendix S1.3 and their distribution over space and relative to atmospheric CO_2 and estimated N deposition is summarized in Figure 1.2. To avoid multicollinearity, all aforementioned predictors were included in a mixed model explaining foliar $\delta^{15}\text{N}$, with ecoregion and species nested within genus as random effects, after which VIF values for each predictor was computed using the `vif` function in the `car` package (Fox & Weisberg, 2018). Predictors with VIF above 3 were sequentially excluded to yield the following set of predictors: log-transformed foliar [N], plant mycorrhizal type, soil N content, soil pH, soil organic carbon, clay and silt fractions, decadal estimates of annual N deposition rates, annual atmospheric CO_2 , herbaceous plant cover, developed land cover (cultivated land cover + built land cover), proportion of EM root stocks, mean annual precipitation, mean annual temperature, latitude, longitude, net primary productivity, plant species, genus, and ecoregion. Source, initial resolution, and units of all original spatial layers are presented in Appendix S1.5.

Spatial foliar $\delta^{15}\text{N}$ analysis: statistical analyses

Species nested within genus and ecoregion were included as random effects to account for non-independence arising from geographic and taxonomic clustering. These effects also

captured differences in $\delta^{15}\text{N}$ arising from differences in plant life form. To test whether foliar $\delta^{15}\text{N}$ diverged by mycorrhizal type depending on variation in CO_2 concentrations or N deposition, we included two-way interactions between plant mycorrhizal type and CO_2 concentrations and plant mycorrhizal type and N deposition rates. Models were fitted using the lmer function in the lme4 package (Bates et al., 2015), with p-values produced using Satterthwaite's approximations of degrees of freedom with the lmerTest package (Kuznetsova et al., 2017).

Results

Herbarium study: mixed models of historical trends in tissue $\delta^{15}\text{N}$ and [N] in Minnesota

Foliar N concentrations in EM and AM plants declined similarly over time in Minnesota ($\text{slope}_{\text{year:AM}}: -0.0019 \pm 0.0004 \text{ \% year}^{-1}$, $p_{\text{AM}} < 0.001$; $\text{slope}_{\text{year:EM}}: 0.0011 \pm 0.0004 \text{ \% year}^{-1}$, $p_{\text{EM}} = 0.009$). Sporocarp [N] also declined in EM fungi ($\text{slope}_{\text{year:EM}}: 0.0016 \pm 0.0007 \text{ \% year}^{-1}$, $p_{\text{EM}} = 0.019$), but remained stable among saprotrophic fungi ($p_{\text{Sap}} = 0.51$), although there was no significant difference between their slopes ($p = 0.25$) (Figure 1.3). EM plants had lower foliar [N] in 1871 compared to AM plants (difference = 0.145 ± 0.073 , $p = 0.038$) and saprotrophic and EM fungi showed no significant differences in modeled [N] in 1871, although saprotrophic fungi trended higher ($p_{\text{fungi}} = 0.683$) (Figure 1.3).

Tissue $\delta^{15}\text{N}$ declined significantly across all groups over time (Figure 1.3). The decline was greatest among AM plants ($-0.043 \pm 0.005\text{‰ year}^{-1}$, $p < 0.001$), followed by EM fungi ($-0.038 \pm 0.007 \text{‰ year}^{-1}$, $p < 0.001$), saprotrophic fungi ($-0.039 \pm 0.009 \text{‰ year}^{-1}$, $p <$

0.001), and EM plants ($-0.028 \pm 0.005 \text{ ‰ year}^{-1}$, $p < 0.001$). The only difference in the slopes emerged among plants: EM foliar $\delta^{15}\text{N}$ declined significantly less than AM foliar $\delta^{15}\text{N}$ ($p = 0.026$) (Figure 1.3).

Spatial foliar $\delta^{15}\text{N}$ analysis: potential controls of foliar $\delta^{15}\text{N}$ and EM fungal N retention across the United States of America

The final model explained 59% of the variation in foliar $\delta^{15}\text{N}$ across the United States (marginal $r^2 = 0.10$ /conditional $r^2 = 0.59$). Foliar $\delta^{15}\text{N}$ was strongly and positively related to foliar N concentrations, and negatively related to atmospheric CO_2 concentrations (Table 1.1). The interaction between mycorrhizal type and N deposition was significant ($p < 0.001$), while the interaction between mycorrhizal type and CO_2 was not. Specifically, AM foliar $\delta^{15}\text{N}$ was significantly and negatively related to N deposition, while EM foliar $\delta^{15}\text{N}$ had no significant relationship with N deposition. Foliar $\delta^{15}\text{N}$ was also significantly related to soil N content, clay fraction, and silt fraction. Further, the proportion of EM root stocks was also strongly negatively related to foliar $\delta^{15}\text{N}$.

Changes in EM foliar ^{15}N depletion across both studies

We calculated differences in foliar $\delta^{15}\text{N}$ between EM and AM plants ($\text{EM } \delta^{15}\text{N} - \text{AM } \delta^{15}\text{N}$; $\delta^{15}\text{N}_{\text{EM-AM}}$) in both datasets. $\delta^{15}\text{N}_{\text{EM-AM}}$ increased from $-3.39 \pm 1.38 \text{ ‰}$ in 1871 ($p = 0.014$) to $-1.27 \pm 1.32 \text{ ‰}$ in 2016 ($p = 0.34$) (Figure 1.4a). Across the United States, we compared EM and AM foliar $\delta^{15}\text{N}$ at the minimum level of N deposition represented in the dataset

(1.8 kg N ha⁻¹ yr⁻¹) and the third quartile level of N deposition (6 kg N ha⁻¹ yr⁻¹) to avoid making predictions at levels of N deposition with low coverage for AM plants (Figure 1.2b). Across the USA, the $\delta^{15}\text{N}_{\text{EM-AM}}$ increased from -1.17 ± 0.44 ‰ at 1.8 kg N ha⁻¹ yr⁻¹ ($p = 0.009$) to 0.06 ± 0.30 ‰ at 6 kg N ha⁻¹ yr⁻¹ ($p = 0.83$) (Figure 1.4b).

Discussion

Both EM and AM plants in Minnesota exhibited comparable declines in foliar [N] over historical increases in atmospheric CO₂ concentrations, despite concomitant N deposition (Figure 1.3). This does not support the hypothesis that AM plants are favored by N deposition because their mode of N acquisition is better adapted to inorganic N environments, which is enhanced under N deposition (Averill et al., 2018). At the same time, our results also do not support the hypothesis that EM plants are advantaged over AM plants in a rising CO₂ world because they have better access to organic N pools (Terrer et al., 2016). Instead, we found that both groups appear increasingly N-limited despite inputs from N deposition. These findings likely reflect that rising CO₂ and N deposition (alongside other environmental shifts that have occurred in Minnesota such as rising temperatures) interact to influence plant N status, complicating predictions from experiments that typically isolate CO₂ and N deposition (Mohan et al., 2014).

We admit that foliar N and $\delta^{15}\text{N}$ are not perfect proxies for plant N status. For example, foliar N concentrations may belie changes in N content (Jonard et al., 2015) or in N use efficiency under changing environmental conditions (B. Smith, 2022). Similarly, foliar

$\delta^{15}\text{N}$ may simply reflect the isotopic composition of deposited N (Hiltbrunner et al., 2019). The design of our study, however, addresses these concerns in two ways: 1) supplementing foliar N trajectories with those of fungal sporocarps and 2) conducting an additional analysis of foliar $\delta^{15}\text{N}$ among EM and AM plants across the US to compare how spatial variation in N deposition and temporal variation in CO_2 concentrations have influenced foliar $\delta^{15}\text{N}$. We show that 1) declining plant [N] was matched by declining [N] in EM fungal sporocarps, consistent with declining N availability over time to plants and the fungi that partially moderate N supply (Figure 1.3). This result represents the first record of declining [N] in EM fungi over historical timescales. We also found that 2) declining foliar $\delta^{15}\text{N}$ was linked to both CO_2 rise and local N deposition, although the latter was true among AM plants alone (Table 1.1). Together, these findings add a new line of evidence for widespread terrestrial N oligotrophication (Mason et al., 2022).

It is possible that long-term trajectories of EM fungal [N] and $\delta^{15}\text{N}$ may not closely track EM foliar [N] and $\delta^{15}\text{N}$. For example, EM fungi have been shown in some cases to constrain N availability to plants through N immobilization (Hasselquist et al., 2016; Näsholm et al., 2013). Under rising CO_2 , inorganic N pools may be insufficient to satisfy increased plant N demand from longer growing seasons and/or increased photosynthesis (CO_2 fertilization effect) (Craine et al., 2018; Elmore et al., 2016), thereby increasing plant reliance on EM fungi for organic N acquisition (Pellitier et al., 2021; Terrer et al., 2016). If rising CO_2 stimulates EM fungal growth, this should increase EM fungal N immobilization and therefore increase plant N limitation, thus decoupling EM plant and

fungal N status when using tissue [N] as an index (Dong et al., 2018). The comparable declines in [N] among EM fungi and plants that we observed, however, are not consistent with this scenario (Figure 1.3). Specifically, both EM fungi and plants exhibit declining [N] over a 40% increase in atmospheric CO₂ concentrations. We stress that our study is situated in temperate forests, which differ from the Fennoscandian boreal forests from which evidence that EM fungi maintain plant N limitation largely derives (P. Högberg et al., 2017).

Tissue $\delta^{15}\text{N}$ declined in both leaves and sporocarps (Figure 1.3). This finding represents the first record of declining $\delta^{15}\text{N}$ in fungal tissues, supplementing similar records from lake sediments, tree rings, and leaves (Mason et al., 2022). Foliar $\delta^{15}\text{N}$ decline, however, was steeper in AM plants than in EM plants in Minnesota. The significant interaction between mycorrhizal type and N deposition rates in the model of foliar $\delta^{15}\text{N}$ across the United States may explain this slope difference (Table 1.1). Specifically, N deposition was negatively related to AM but not EM $\delta^{15}\text{N}$ (Table 1.1). This interaction may arise from differences in N source: if deposited N is low in $\delta^{15}\text{N}$, this signal may show up faster in AM plants relying on “newer” inorganic N compared to EM plants acquiring significant portions of their N from older, organic sources. This explanation is complicated by evidence that plant tissue $\delta^{15}\text{N}$ does not reflect the isotopic signature of deposited N, but instead may reflect N deposition-mediated changes in soil biogeochemical processes (Savard et al., 2023). Indeed, this interaction, which resulted in a reduction of the ^{15}N depletion characteristic of EM leaves relative to AM leaves (Figure 1.4b), may reflect a change in EM N transfer

dynamics that reduces the ^{15}N depletion in foliar N. If plants obtain a smaller proportion of N from EM fungi or EM fungal N retention in mycelia decreases, foliar ^{15}N depletion in EM plants should decrease (Hobbie & Högberg, 2012). Both of these explanations would be plausible under N deposition, which may reduce EM plant reliance on organic N acquired by EM fungi, or reduce EM fungal growth, lessening N sequestrations in non-mobile pools that drive ^{15}N depletion in foliar N (Hobbie & Högberg, 2012; Lilleskov et al., 2002, 2019).

The stability of the [N] of saprotrophic fungal sporocarps over 14 decades is intriguing. Historical declines in plant tissue $\delta^{15}\text{N}$ are often attributed to decreased soil N availability limiting the microbial activities that drive soil ^{15}N enrichment (Craine et al., 2015). Organisms relying on soil N like saprotrophic fungi may then exhibit declining N status over time. In our data, however, this was not the case. It is important to note that of the 71 saprotrophic fungal specimens analyzed in this study, the two best represented species (*Lycoperdon pyriforme* and *Psathyrella candolleana*, $n = 31$) are wood rotters. Because these fungi were likely reliant on wood for N supply, their N trajectories may not track soil N availability. Terrestrial saprotrophs may be more sensitive to changes in soil N availability; however, investigating this further was not possible in this study given limited species-level collections. Future study of saprotrophic fungal N trajectories over time at the species level should help to better understand how decomposers that both moderate and are subject to changing soil N availability have responded to historical environmental change.

Conclusions

Herbarium specimens contain rich information about ecosystem responses to historical environmental change. By analyzing collections from a region that has experienced concomitant atmospheric N deposition and CO₂ rise, we found that foliar N trajectories did not diverge by mycorrhizal type as expected from results based on short-term experimentation. Instead, EM fungi as well as EM and AM plants exhibited declining tissue N concentrations despite regional N deposition, adding a new line of evidence in support of widespread terrestrial N oligotrophication (Mason et al., 2022). Smaller declines in EM foliar $\delta^{15}\text{N}$ than in AM foliar $\delta^{15}\text{N}$ in Minnesota may be explained by divergent responses to N deposition, evidenced by the significant interaction between N deposition and mycorrhizal type in the reanalysis of previously published foliar $\delta^{15}\text{N}$ data from across the USA. These differential responses likely reflect differences in N acquisition between mycorrhizal types and warrant further investigation.

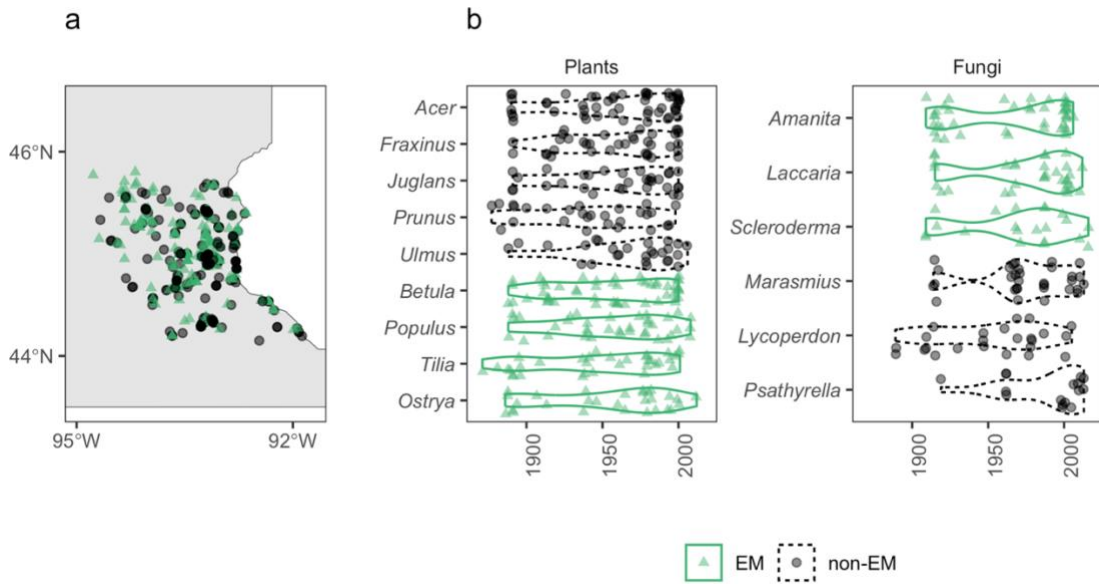


Figure 1.1. Summary of foliar and sporocarp samples from herbarium collections made in Minnesota, USA, from 1871 to 2016. (a) Spatial distribution of ectomycorrhizal (EM) and non-EM collections with exact coordinate information. (b) Genus-level collections of arbuscular mycorrhizal (AM) and EM plants and EM and saprotrophic fungi across time. Black circles, dotted line = non-EM; green triangles, solid line = EM.

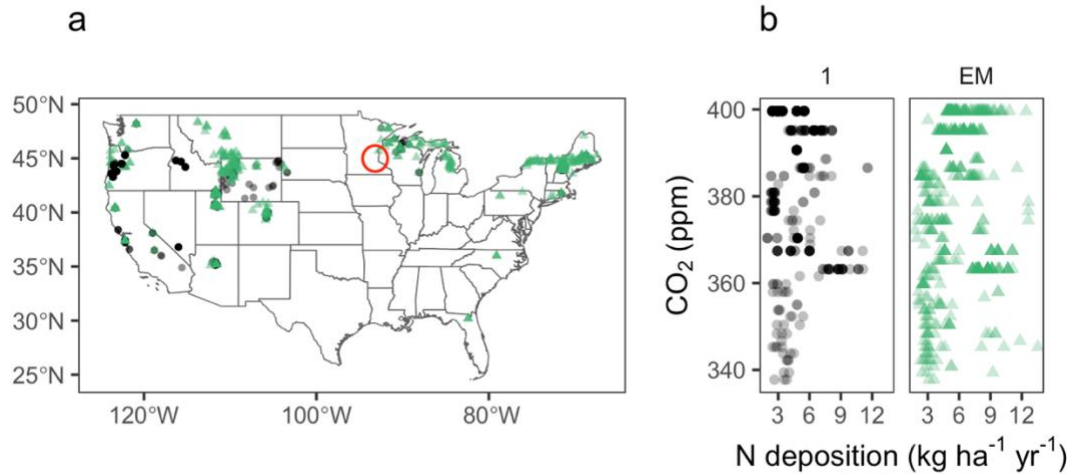


Figure 1.2. Summary of foliar data compiled by Craine et al. (2018) from arbuscular mycorrhizal (AM) and ectomycorrhizal (EM) plants analyzed (a) across the United States (red circle indicates the location of samples from Minnesota) and (b) with reference to contemporaneous atmospheric carbon dioxide (CO₂) concentrations and annual nitrogen (N) deposition rates. Black circles = AM plants; green triangles = EM plants

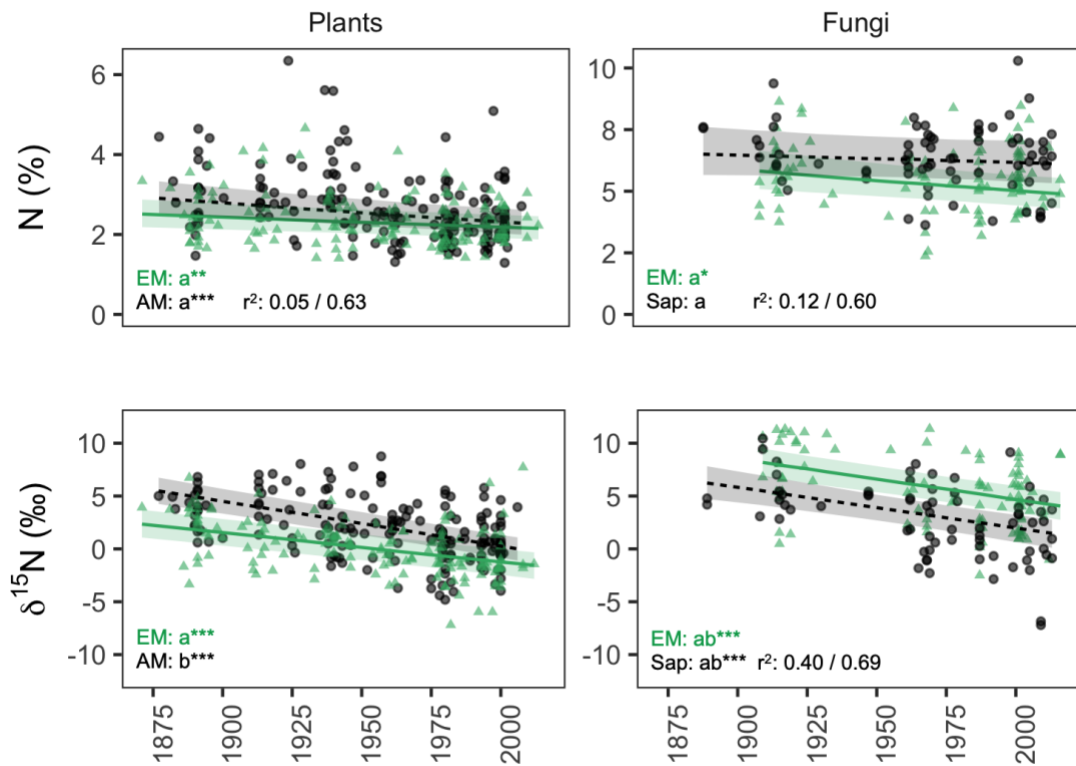


Figure 1.3. Temporal trends in measured and modeled $[N]$ and $\delta^{15}N$ among ectomycorrhizal (EM) plants, arbuscular mycorrhizal (AM) plants, EM fungi, and saprotrophic (Sap) fungi with 80% prediction intervals associated with fixed effects. Asterisks indicate significant temporal trends (*, $P < 0.05$; **, $P < 0.01$; ***, $P < 0.001$), while letters denote differences in slope between groups. Green triangles, solid line = EM; black circles, dotted line = non-EM. Marginal and conditional r^2 values are given for each of the three models (plant $[N]$, fungal $[N]$, and $\delta^{15}N$) in the bottom right of the corresponding panels.

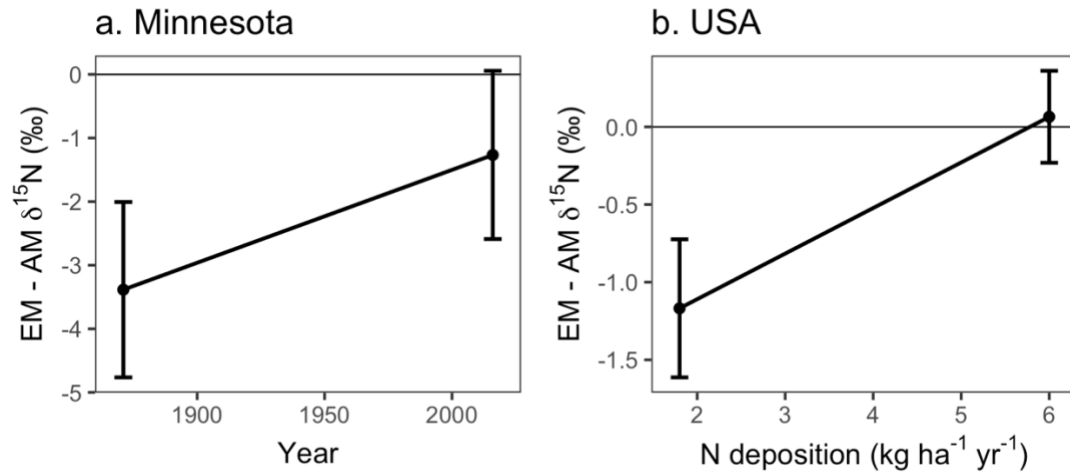


Figure 1.4. Changes in ^{15}N depletion in ectomycorrhizal (EM) versus arbuscular mycorrhizal (AM) leaves across (a) 145 year environmental change in Minnesota, USA (b) atmospheric nitrogen deposition rates across the United States. Error bars represent standard errors, estimated using the function `ggeffect` in the `GGEFFECTS` package (Ludecke, 2018).

Table 1.1. Summary of fixed effects in mixed model of ectomycorrhizal (EM) and arbuscular mycorrhizal (AM) foliar $\delta^{15}\text{N}$ across the United States (using data from Craine et al. 2018), grouped by climate features (MAP = mean annual precipitation, MAT = mean annual temperature, NPP = net primary productivity), land cover features (Herbaceous = herbaceous land cover, Developed = built and agricultural land cover, EM Root Stock Proportion = proportion of EM root stocks), location, edaphic features, plant features (log(Leaf N) = log-transformed leaf nitrogen concentrations, MT: AM = arbuscular mycorrhizal, MT: EM = ectomycorrhizal), global change drivers, and interactions between global change drivers (N deposition = nitrogen deposition, CO_2 = atmospheric carbon dioxide) and mycorrhizal type. Significant factors are bolded, significant interactions are indicated by superscript letters.

Predictor	Estimate	Standard error	p value
MAP	5.73E-04	5.29E-04	0.280
MAT	9.55E-02	5.84E-02	0.103
NPP	1.50E-04	1.67E-04	0.369
Herbaceous Cover	7.51E-03	1.15E-02	0.514
Developed Land Cover	5.09E-03	9.43E-03	0.590
EM Root Stock Proportion	-1.26	4.32E-01	0.004
Latitude	1.91E-02	8.54E-02	0.823
Longitude	-2.31E-03	2.39E-02	0.924
Soil N Content	-3.12E-03	1.15E-03	0.007
Soil Organic Carbon Stock	1.28E-03	7.10E-04	0.072
Soil pH	4.89E-02	2.75E-02	0.076
Soil Clay Fraction	-7.93E-03	2.34E-03	0.001
Soil Silt Fraction	4.92E-03	1.89E-03	0.010
log(Leaf Nitrogen Concentration)	3.89	4.98E-01	< 0.001
MT: AM	7.53	6.36	0.237
MT: EM	1.85E-01	5.62	0.974
N Deposition X MT: AM^a	-3.09E-01	1.02E-01	0.002
N Deposition X MT: EM ^b	-1.43E-03	8.74E-02	0.987
CO_2 X MT: AM^a	-4.49E-02	1.16E-02	< 0.001
CO_2 X MT: EM^a	-3.02E-02	7.69E-03	< 0.001

Chapter 2

Carbon cycling through plant and fungal herbarium specimens tracks the Suess effect over more than a century of environmental change

Summary

Although the anthropogenic decline in atmospheric carbon stable isotope ratios ($\delta^{13}\text{C}$) over the last 150 years (termed the Suess effect) is well-studied, how different terrestrial trophic levels and modes reflect this decline remains unresolved. To evaluate the Suess effect as an opportunistic tracer of terrestrial forest carbon cycling, this study analyzed the $\delta^{13}\text{C}$ in herbarium specimens collected in Minnesota, USA from 1877-2019. Our results suggest that both broadleaf trees and ectomycorrhizal fungi relied on recent photosynthate to produce leaves and sporocarps, while saprotrophic fungi on average used carbon fixed from the atmosphere 32-55 years ago for sporocarp construction. The $\delta^{13}\text{C}$ values of saprotrophic fungal collections were also sensitive to the age of their plant carbon substrate, with sporocarps of twig specialists tracking changes in atmospheric $\delta^{13}\text{C}$ more closely than saprotrophs growing on logs. Collectively, this study indicates that natural history collections can quantitatively track carbon cycling among plants and fungi over time.

Introduction

Anthropogenic carbon emissions have progressively labeled the atmosphere with isotopically light carbon (^{12}C) over the past two centuries. This is primarily due to the burning of fossil fuels, which are ^{13}C -depleted and thus impart a greater light carbon signature on the atmosphere (Keeling, 1979). From 1877 to 2019, atmospheric $\delta^{13}\text{C}$ (the ratio of ^{13}C to ^{12}C compared to the ratio in the reference standard) dropped by approximately 1.9‰ (Keeling, 1979; Belmecheri and Lavergne, 2020). This overall trend is actually best described by a piecewise linear function, characterized by a gradual decline from approximately 1850 until 1957, and a steeper decline thereafter (Belmecheri & Lavergne, 2020). These differing rates of decline coincide closely with global carbon dioxide emissions, which increased five-fold from 1957 to 2022 (R. M. Andrew & Peters, 2023).

The anthropogenic change in atmospheric $\delta^{13}\text{C}$, termed the Suess effect, serves as an opportunistic label that can be tracked over time through isotopic analysis of natural history collections. For example, studies of marine organisms (corals, reef fishes) have shown consistent changes in tissue $\delta^{13}\text{C}$ that closely tracked the incorporation of progressively lighter C (more ^{12}C) in recent decades (Swart et al., 2010; Sabadel et al., 2020). While this effect is relatively widely recognized in marine ecosystems, how it manifests in terrestrial systems is less well documented (Hobbie et al., 2020). Testing whether the Suess effect manifests across different trophic levels and trophic modes is particularly important, as it will reflect the rate at which carbon moves into and through terrestrial ecosystems.

Fungi, as heterotrophs, have diverse trophic modes that affect how and when they assimilate photosynthetically-derived carbon. Ectomycorrhizal fungi are functionally obligate symbionts of plants and are characterized by their dependence on recent photosynthate (Högberg et al., 2010; Smith and Read, 2010; Hobbie et al., 2021), while saprotrophic fungi assimilate carbon from dead organic matter of variable ages (Hobbie et al., 2002, 2016, 2020; Newsham et al., 2018). These aspects of their ecology should affect their temporal $\delta^{13}\text{C}$ trends: ectomycorrhizal fungi should closely track the isotopic composition of photosynthate, while saprotrophic fungal $\delta^{13}\text{C}$ should mirror the composition of their substrate (e.g. leaf litter, logs, twigs).

Based on differing rates of decline in atmospheric $\delta^{13}\text{C}$ over the past 150 years, the isotopic composition of leaves produced by broadleaf trees, which incorporate recent photosynthate and stored carbon (Gaudinski et al., 2009; Muhr et al., 2016), should decline more steeply after 1957. Accordingly, ectomycorrhizal fungal $\delta^{13}\text{C}$, relying predominantly on photosynthate, should also decline more steeply after 1957. The point at which saprotrophic fungal $\delta^{13}\text{C}$ declines more steeply should reflect the average age of their substrate, providing a novel estimate of the age of fungal-available carbon in organic matter. For example, the overall decline in $\delta^{13}\text{C}$ should be less among saprotrophic fungi growing on older substrates (i.e., logs) than newer substrates (i.e., twigs), reflecting the slower decline in atmospheric $\delta^{13}\text{C}$ before 1957.

To evaluate these predictions, we analyzed the isotopic composition of 561 plant and fungal samples collected in Minnesota, USA between 1877 to 2019. First, we fit mixed

linear models with appropriate random effects to evaluate whether $\delta^{13}\text{C}$ declined more quickly in plants and ectomycorrhizal fungi than in saprotrophic fungi. We then fit piecewise linear models to plant and fungal $\delta^{13}\text{C}$ and compared breakpoint values for recent photosynthate relative to saprotrophic fungi to estimate the average age of saprotrophic fungal carbon. Finally, we used a mixed linear model to assess whether $\delta^{13}\text{C}$ trends of saprotrophic fungi growing on twigs had a steeper negative slope than those growing on logs. Collectively, these analyses allow for quantitative estimates of the movement of carbon from the atmosphere through various forest trophic pools.

Materials and Methods

Sample Selection

Plant (n = 286) and fungal (n = 275) specimens collected in Minnesota from 1877-2019 were selected from the Bell Herbarium at the University of Minnesota. Plant collections represent eight common genera of woody plants (*Acer*, *Betula*, *Fraxinus*, *Juglans*, *Populus*, *Prunus*, *Tilia*, and *Ulmus*). The 109 ectomycorrhizal fungal specimens represent three common genera (*Amanita*, *Laccaria*, and *Scleroderma*). Of the 166 saprotrophic fungal collections, six genera are represented (*Cerioporus*, *Lycoperdon*, *Marasmius*, *Neofavolus*, *Phellinus*, and *Trichaptum*). Saprotrophic fungi specific to logs include *Trichaptum biforme*, *Phellinus gilvus*, and *Lycoperdon pyriforme*. Twig specialists include *Neofavolus alveolaris* and *Cerioporus leptcephalus* (Bessette et al., 1997; Kuo & Methven, 2014). Habitat descriptions of collections were referenced to confirm substrate specificity. Further information about sampling is available in Table 2.1.

Elemental and Isotopic Analysis

Air-dried foliar and sporocarp tissues were ground and packed at a mass of 1.2 ± 0.05 mg to the nearest 0.001 mg. Due to a multi-stage process of data generation, samples were analyzed at three different facilities. Samples were analyzed via an Elementar Vario Pyrocube (Hanau, Germany) interfaced to an Isoprime 100 isotope ratio mass spectrometer (Cheadle, UK) at the University of Minnesota, an Elementar Vario EL Cube interfaced to a PDZ Europa 20-20 isotope ratio mass spectrometer (Sercon Ltd., Cheshire, UK) at the University of California-Davis Stable Isotope Facility, or an Elementar Cube elemental analyzer interfaced to a GV Instruments Isoprime isotope ratio mass spectrometer (Manchester, UK) at Boston University Stable Isotope Laboratory. Samples at all facilities were run with internal control standards to ensure comparable data quality and comparisons of ^{15}N from a subset of the same specimens revealed no effect of facility on the obtained values (Michaud et al. 2023).

Statistical Analyses

All statistical analyses were performed in R (version 4.1.2, R Core Team, 2021). Historical estimates of atmospheric $\delta^{13}\text{C}$ were compiled from Belmecheri and Lavergne (2020). To assess differences in the slope of $\delta^{13}\text{C}$ over time among plants, ectomycorrhizal fungi, and saprotrophic fungi, a linear mixed model was constructed using the lme4 and lmerTest packages (Bates et al., 2015; Kuznetsova et al., 2017) with random effects accounting for location (collection county), taxonomy (genus), and seasonality (month collected).

Random effects were then backwards selected using the Akaike information criterion (AIC, threshold = 2) with the “step” function (base package) preserving genus alone. Group (plant, ectomycorrhizal fungus, saprotrophic fungus), year, and their interaction were included as fixed effects.

To assess the potential for differing rates of $\delta^{13}\text{C}$ decline over time, we investigated whether there was a breakpoint in $\delta^{13}\text{C}$, i.e. when the slope of $\delta^{13}\text{C}$ decline was estimated to change, for atmospheric $\delta^{13}\text{C}$ and for each group. To estimate the breakpoint for atmospheric $\delta^{13}\text{C}$ based on the data of Belmecheri and Lavergne (2020), we used the “segmented” function in the segmented package on a linear model fit with interpolated $\delta^{13}\text{C}$ as the response variable and year as the independent variable, indicating that year was the variable to segment. For each group, a segmented or piecewise linear model was fit by first fitting a mixed linear model (Bates et al., 2015; Kuznetsova et al., 2017) with month, genus, and county as random effects and year as a fixed effect, performing backwards AIC selection on random effects to fit more parsimonious models, and then regressing the partial residuals from the reduced mixed model related to year against year using “lm” (base package). A piecewise linear model was then fit using the function “segmented” (segmented package) (Muggeo, 2008) to estimate the most probable year at which the slope of $\delta^{13}\text{C}$ changed. The “conf.interval” function was used to produce confidence intervals and standard errors around the estimated breakpoints for each group. This enabled testing the differences among $\delta^{13}\text{C}$ breakpoints in plants, ectomycorrhizal fungi, and saprotrophic fungi via z-tests.

A subset of saprotrophic fungi were also used to test whether substrate age was linked with carbon age. Specifically, we identified saprotrophic fungi specific to logs and trunks (*Lycoperdon pyriforme*, n = 19, *Phellinus gilvus*, n = 23, *Trichaptum biforme*, n = 35) versus those growing on small branches and twigs (*Cerioporus leptcephalus*, n = 16; *Neofavolus alverolaris*, n = 20). Substrate specificity was also verified via observational notes included in the record collections. Potential differences in temporal $\delta^{13}\text{C}$ trends were tested using a linear mixed effects model (Bates et al., 2015; Kuznetsova et al., 2017). To test for slope differences reflecting substrate age, the model included a fixed term representing time (year collected) with an interaction between substrate (log or twig) and year. Random effects accounting for differences in taxonomy (species), and location (county of collection) were backwards AIC selected, yielding species alone as a random effect.

Results

Historical declines in atmospheric, plant, and fungal $\delta^{13}\text{C}$

As noted above, atmospheric $\delta^{13}\text{C}$ declined by 1.9‰ from 1877 to 2019 (Belmecheri and Lavergne 2020). Mixed linear modeling estimated that over the same period foliar $\delta^{13}\text{C}$ declined 3.5‰ on average ($-0.024 \pm 0.002\text{‰ yr}^{-1}$, $t = -12.108$, $p < 0.001$), from -25.8‰ (95% CI: -26.4‰ to -25.3‰) to -29.3‰ (-29.8‰ to -28.8‰). Ectomycorrhizal fungal $\delta^{13}\text{C}$ declined by 2.4‰ on average ($-0.017 \pm 0.004\text{‰ yr}^{-1}$, $t = -4.776$, $p < 0.001$), from -22.7‰

(-23.6‰ to -21.9‰) to -25.6‰ (-26.3‰ to -24.8‰), while saprotrophic fungal $\delta^{13}\text{C}$ declined 1.1‰ on average ($-0.008 \pm 0.003\text{‰ yr}^{-1}$, $t = -2.984$, $p = 0.003$), from -22.7 (-23.4‰ to -22.0‰) to -23.8‰ (-24.4‰ to -23.2‰). Overall, the model explained 75.6% of the variation in the data (marginal $r^2 = 0.698$, conditional $r^2 = 0.756$). These declines differed significantly across groups, with saprotrophic fungal $\delta^{13}\text{C}$ declining significantly less than in plants ($t = -4.914$, $p < 0.001$) and in ectomycorrhizal fungi ($t = -1.986$, $p = 0.048$) (Figure 2.1). Additionally, ectomycorrhizal fungal $\delta^{13}\text{C}$ declined less than in plants, although this trend was marginally significant ($t = -1.907$, $p = 0.057$).

Breakpoint differences between atmospheric, foliar, and fungal $\delta^{13}\text{C}$

A significant breakpoint, or the most probable year in which the slope of $\delta^{13}\text{C}$ decline changed, was detected in atmospheric $\delta^{13}\text{C}$ between 1956-1957 ($r^2 = 0.99$, 95% CI: 1956.2 – 1957.5, $p < 0.001$), consistent with separating an early period of shallow $\delta^{13}\text{C}$ decline from a later steep decline (Figure 2.2A). In plants, after accounting for variation arising from the month of the collection and plant genus, a breakpoint was detected in 1957 ($r^2 = 0.31$, 1932.0–1982.0, $p = 0.013$) (Figure 2.2B). In saprotrophic fungi, a marginally significant breakpoint was estimated at 2001 ($r^2 = 0.09$, 1989.2 – 2012.9, $p = 0.087$), after accounting for non-independence arising from genus identity (Figure 2.2D). The breakpoint in $\delta^{13}\text{C}$ in saprotrophic fungi was significantly later than for the atmosphere and plants ($z = -7.351$, $p < 0.001$; $z = -3.129$, $p < 0.001$), while the breakpoint in plants was comparable to that in the atmosphere ($z = -0.013$, $p = 0.494$) (Figure 2.2). In ectomycorrhizal fungi, after accounting for the same sources of potential non-

independence, no significant breakpoint was detected ($p = 0.652$, Figure 2.2C). Comparing the earlier and later slopes of saprotrophic fungi, plants, and the atmosphere revealed no significant differences based on 95% confidence intervals (Appendix S2.1).

Difference in $\delta^{13}\text{C}$ trend among twig and log rotters

In log-rotting saprotrophic fungi, $\delta^{13}\text{C}$ did not decline significantly over time ($p = 0.139$). In twig-rotting saprotroph fungi, however, $\delta^{13}\text{C}$ declined 2.2‰ on average ($-0.015 \pm 0.004\text{‰ yr}^{-1}$, $t = -3.862$, $p < 0.001$) from -22.8‰ in 1877 (-23.8‰ to -21.8‰) to -25.0‰ in 2019 (-25.9‰ to -24.1‰). Comparing these two groups, the slope of $\delta^{13}\text{C}$ among log saprotrophs was significantly different from that of twig saprotrophs ($t = 2.115$, $p = 0.037$, Figure 2.3). This model explained 35.9% of the variation in $\delta^{13}\text{C}$ (marginal $r^2 = 0.207$, conditional $r^2 = 0.359$)

Discussion

In this study, we evaluated whether the Suess effect generated an opportunistic isotopic label in plant and fungal herbarium specimens that could track various aspects of terrestrial carbon cycling. Specifically, we compared 1) cumulative declines in $\delta^{13}\text{C}$ across broadleaf trees, ectomycorrhizal fungi, and saprotrophic fungi, 2) breakpoint estimates in $\delta^{13}\text{C}$ across the three groups, and 3) cumulative declines in $\delta^{13}\text{C}$ across saprotrophic fungi specializing on substrates of different ages (twigs versus logs). In line with our expectations, we found evidence that the Suess effect generated a strong isotopic signal in the carbon of both plant and fungal herbarium specimens. Our results indicated that leaves of broadleaved plants

and ectomycorrhizal fungal sporocarps contained very recent carbon while sporocarps of saprotrophic fungi were built from carbon fixed 44 years prior to collection on average (i.e. saprotrophic fungal $\delta^{13}\text{C}$ breakpoint minus that of the atmosphere). Furthermore, among saprotrophs, $\delta^{13}\text{C}$ trends differed with substrate age, with twig-rotters reflecting the steep decline in atmospheric $\delta^{13}\text{C}$ since 1957 unlike log-rotters.

While the analysis of $\delta^{13}\text{C}$ breakpoints requires high sample size given data noisiness, our results suggest that this approach offers a novel method of estimating the age of fungal and plant carbon. Breakpoint analysis has been previously used with $\delta^{15}\text{N}$ values from herbarium specimens to approximate the onset of $\delta^{15}\text{N}$ decline in leaves (McLauchlan et al., 2010); this study extends its usage to natural abundance $\delta^{13}\text{C}$, taking advantage of the piecewise decline in atmospheric $\delta^{13}\text{C}$ to estimate carbon age in both fungi and plants. The breakpoint detected in atmospheric $\delta^{13}\text{C}$ around 1957 was similar for plants, which is consistent with plant reliance on recent photosynthate to construct leaves (Gaudinski et al., 2009). In contrast, the 32-55 year delay in the breakpoint of saprotrophic fungi suggests a significant lag between when carbon is fixed from the atmosphere by plants and the production of fungal sporocarps resulting from its decomposition (Hobbie et al., 2016, 2020). We emphasize that the length of delay depends on the portion of the saprotrophic community sampled, which in our case was strongly biased towards wood-rotting fungi. Dendrochronological analysis reveals that wood $\delta^{13}\text{C}$ declines over time, supporting that wood $\delta^{13}\text{C}$ mirrors atmospheric $\delta^{13}\text{C}$ (Leavitt and Lara, 1994; Arneeth et al., 2002;

Robertson et al., 2004; Bassett et al., 2023), and passes that signature onto the fungi that decompose it.

The lack of a breakpoint among ectomycorrhizal fungi was surprising given the similar Suess effect trends between this fungal guild and plants. We suspect this absence may be due to differences in data composition; relative to plants, the ectomycorrhizal fungal samples were less numerous and absent between 1935 and 1955, the two decades prior to the $\delta^{13}\text{C}$ breakpoint that emerges in the atmosphere. The lack of a breakpoint may alternatively reflect differences in organic nitrogen (N) acquisition ability among ectomycorrhizal fungal species. In previous studies, ectomycorrhizal fungi varied considerably in their use of organic N, which contains carbon with higher $\delta^{13}\text{C}$ (Hobbie et al., 2013; Chen et al., 2016; Vaario et al., 2019). Incorporation of organic N may therefore obscure temporal trends when analyzed in aggregate, explaining why ectomycorrhizal fungal $\delta^{13}\text{C}$ does not directly match photosynthate or atmospheric $\delta^{13}\text{C}$. This interpretation is bolstered somewhat by the marginally steeper decline in $\delta^{13}\text{C}$ among plants compared to ectomycorrhizal fungi that may reflect incorporation of older, ^{13}C -enriched carbon among some taxa. Alternatively, if any of the ectomycorrhizal fungi sampled were associated with trees not included in this study, then the $\delta^{13}\text{C}$ of those trees and the photosynthate passed to the ectomycorrhizal fungi could differ from the trees we measured.

Our comparison of twig-rotting fungi versus log-rotting fungi is also consistent with the time-dependent nature of saprotrophic fungal $\delta^{13}\text{C}$. In line with the timing of plant tissue construction, the steeper decline in $\delta^{13}\text{C}$ over time among twig-rotters compared to log-

rotters reflects that twig-rotters build sporocarps with more recently fixed carbon compared to log-rotters, thus indexing over more recent, steeper declines in atmospheric $\delta^{13}\text{C}$. Logs contain many more years of carbon accumulation than twigs, leading us to hypothesize that log-rotting fungi would decline less in $\delta^{13}\text{C}$ than twig-rotting fungi. Their $\delta^{13}\text{C}$ did not decline at all. Given that this result emerged, we are confident that $\delta^{13}\text{C}$ in saprotrophic fungal collections is sensitive enough to track historical carbon cycling, opening a novel line of research. For example, differences in rates of organic matter decomposition could presumably be compared over geographic space using historical collections of the same fungal species. Additionally, this approach could be used with species-level collections of ectomycorrhizal fungi to assess differences in organic nitrogen use. The $\delta^{13}\text{C}$ of caps (high in protein) versus stipes (low in protein) of individual sporocarps could be compared over time, with a hypothesized greater ^{13}C enrichment of caps in more recent collections reflecting a greater ^{13}C enrichment of soil-derived organic N relative to recent photosynthate.

Collectively, our findings indicate that natural abundance $\delta^{13}\text{C}$ in preserved herbarium specimens is sensitive to the Suess effect, allowing us to track carbon age and cycling over historical timescales. Notably, our results highlight that broadleaf trees and ectomycorrhizal fungi build leaves and sporocarps with more recently fixed carbon than that in sporocarps of saprotrophic fungi. This finding, while not novel, demonstrates that the Suess effect can be used to track carbon cycling via longitudinal surveys of plant and fungal herbarium specimens. Given this demonstrated sensitivity, we encourage the use of

natural history collections in conjunction with experimental studies to better understand terrestrial carbon cycling dynamics across different time scales.

Table 2.1. Genus-level summary of collections analyzed in this study with reference to their ecological group (Sap: saprotrophic fungus, Ecto = ectomycorrhizal fungus, Plant = broadleaf tree), genus, number of species sampled in each genus (Species), and number of collections (Count).

group	Genus	Species	Count
Sap	<i>Cerioporus</i>	1	16
Sap	<i>Lycoperdon</i>	12	36
Sap	<i>Marasmius</i>	10	36
Sap	<i>Neofavolus</i>	1	20
Sap	<i>Phellinus</i>	1	23
Sap	<i>Trichaptum</i>	1	35
Ecto	<i>Amanita</i>	8	47
Ecto	<i>Laccaria</i>	8	37
Ecto	<i>Scleroderma</i>	8	25
Plant	<i>Acer</i>	3	51
Plant	<i>Betula</i>	4	51
Plant	<i>Fraxinus</i>	1	36
Plant	<i>Juglans</i>	2	23
Plant	<i>Populus</i>	2	36
Plant	<i>Prunus</i>	1	28
Plant	<i>Tilia</i>	1	34
Plant	<i>Ulmus</i>	2	27

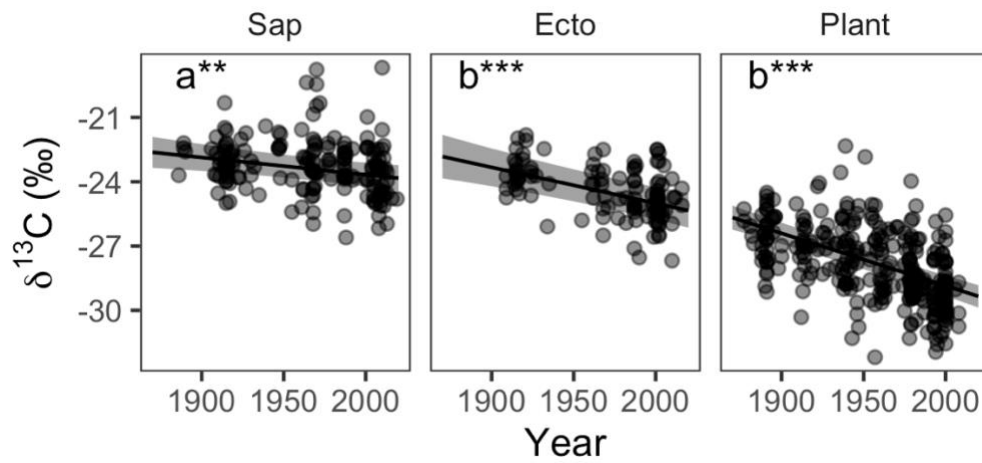


Figure 2.1. Trends in tissue $\delta^{13}\text{C}$ among herbarium specimens, including saprotrophic (Sap) fungal sporocarps, ectomycorrhizal (Ecto) fungal sporocarps, and plant leaves over time. Letters denote significant slope differences, while the asterisks denote the significance of the trend (***: $p < 0.001$, **: $p < 0.01$).

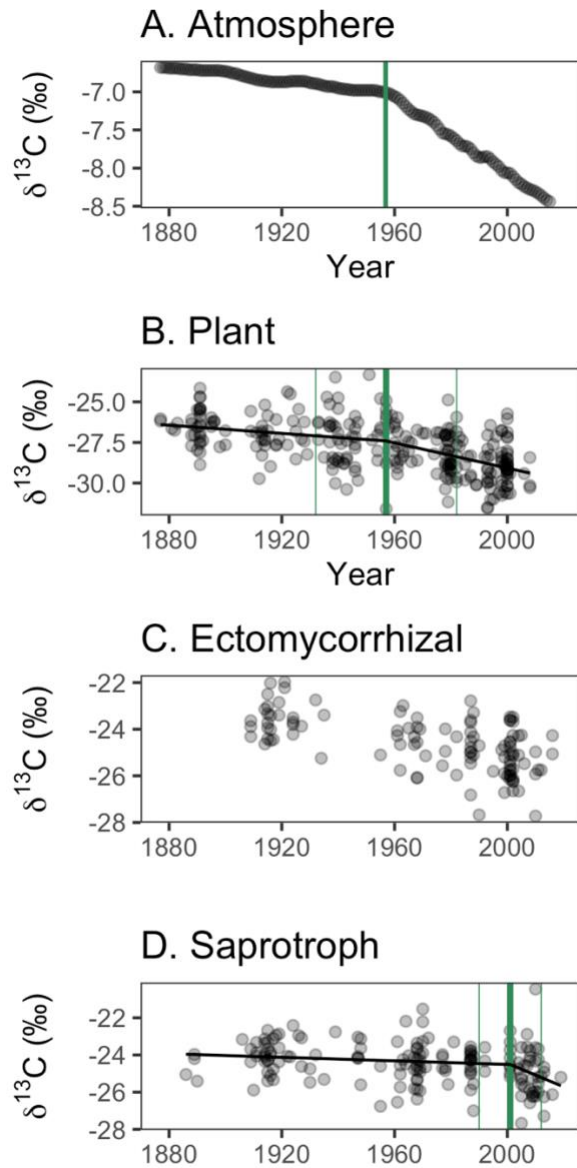


Figure 2.2. Trends in tissue $\delta^{13}\text{C}$ over 14 decades. Differences in $\delta^{13}\text{C}$ breakpoint estimates are illustrated in green among (A) the atmosphere, (B) broadleaf trees, (C) ectomycorrhizal fungi, and (D) saprotrophic fungi (thick line = breakpoint estimate, thin lines = 95% confidence interval around estimate).

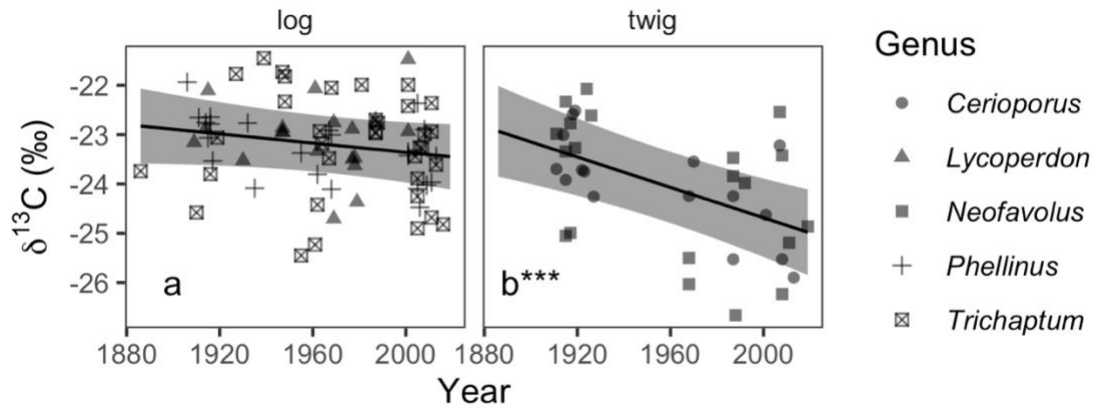


Figure 2.3. Patterns in the $\delta^{13}\text{C}$ decline over time of twig-rotting and log-rotting saprotrophic fungi, with 95% confidence intervals around the mean line. Letters denote significant slope differences, while the asterisks denote the significance of the trend (***: $p < 0.001$). Point shapes correspond to fungal genus.

Chapter 3

Mast seeding in European beech (*Fagus sylvatica* L.) is associated with reduced fungal sporocarp production and community diversity

Summary

Mast seeding is a well-documented phenomenon across diverse forest ecosystems. While its effect on aboveground food webs has been thoroughly studied, how it impacts the soil fungi that drive soil carbon and nutrient cycling have not yet been explored. To evaluate the relationship between mast seeding and fungal resource availability, we paired a Swiss 29-year fungal sporocarp census with contemporaneous seed production for European beech (*Fagus sylvatica* L.). On average, mast seeding was associated with a 55% reduction in sporocarp production and a compositional community shift towards drought-tolerant taxa across both ectomycorrhizal and saprotrophic guilds. Among ectomycorrhizal fungi, traits associated with carbon cost did not explain species' sensitivity to seed production. Together, our results support a novel hypothesis that mast seeding limits annual resource availability and reproductive investment in soil fungi, creating an ecosystem 'rhythm' to forest processes that is synchronized above- and belowground.

Introduction

Mast seeding, or the synchronous production of an outsized seed crop in a population of plants, is a well-documented global phenomenon (Kelly, 1994). Mast seeding is often investigated as a resource input, wherein large seed crops increase the local abundance of seed predators (Bogdziewicz et al., 2016) and are a labile substrate for decomposers (Zackrisson et al., 1999), frequently causing cascading effects on food webs (Ostfeld et al., 2000). The altered fate of the resources necessary to produce a mast seed crop – including water, nitrogen, and carbon – also causes resource limitation within the mast seeding plant (Pearse et al., 2016). Many tree species switch resources away from vegetative growth to produce a mast seed crop (Pearse et al., 2016), evidenced by negative correlations between tree ring growth and seed production (Koenig & Knops, 1998). In a mast year, the flux of resources redirected towards seed production may limit resource availability to organisms that are dependent on trees or soil from which the trees draw resources.

Forest-dwelling fungi span many ecological niches and are often categorized according to their trophic mode or guild. For instance, saprotrophic fungi decompose a variety of organic matter types, while root-associated ectomycorrhizal fungi are sustained by a combination of photosynthate from host plants and nutrients held in soil inorganic and organic matter (S. E. Smith & Read, 2010). Their complementary life cycles drive forest nutrient cycling globally (Baldrian et al., 2023): saprotrophic fungi possess uniquely powerful mechanisms that degrade recalcitrant organic matter (Baldrian, 2008), while

mycorrhizal fungi mediate the transfer of nutrients to trees (Hoeksema et al., 2010; Näsholm et al., 2013), thereby influencing primary productivity.

These differences may determine their sensitivity to mast seeding events. Because ectomycorrhizal fungi are dependent on trees for carbon, we anticipate that ectomycorrhizal fungi will be more sensitive to mast seed production than saprotrophic fungi. Like mast seed crops, ectomycorrhizal sporocarp production depends on recent photosynthate (Hobbie et al., 2021; P. Högberg et al., 2001). Accordingly, ectomycorrhizal fungi appear more proximally affected by tree resource availability compared to saprotrophic fungi: Collado et al. (2018) found that ectomycorrhizal sporocarp production was correlated with vegetative growth of trees in that year, while saprotrophic sporocarp production was linked with growth two years earlier. Additionally, ectomycorrhizal fungal sporocarp production is typically more seasonal than sporocarp production of saprotrophic fungi, evidenced by a unimodal peak in sporocarp production during peak tree productivity compared to the more stable pattern of production across the season among saprotrophs (Ponce et al., 2023; Sato et al., 2012). Resource switching during masting may reduce resource allocation belowground (Nikolova et al., 2011), or require increased nitrogen and/or water uptake by trees (Pearse et al., 2016), both of which may more immediately affect ectomycorrhizal fungi than saprotrophic fungi (Kranabetter et al., 2019).

Ectomycorrhizal fungal activity and root presence, however, can influence saprotrophic fungal activity (Frey, 2019). For instance, ectomycorrhizal fungal activity is posited to

reduce saprotrophic fungal activity through competition for nitrogen and/or water in the same substrates when resources are sufficiently scarce, a phenomenon commonly referred to as the ‘Gadgil effect’ (Fernandez & Kennedy, 2016; Gadgil & Gadgil, 1971). Roots, on the other hand, may prime saprotrophic fungal activity by exuding labile carbon-containing compounds (Dijkstra et al., 2013; Huo et al., 2017). Thus, if during a mast year, trees decrease belowground carbon allocation and/or increase nitrogen and water uptake facilitated by ectomycorrhizal fungi, this may reduce resource availability to saprotrophic fungi, despite their ‘free-living’ designation.

Ectomycorrhizal fungi also differ in the magnitude of their own resource demand (Bidartondo et al., 2001; Hobbie & Colpaert, 2003), which may influence their sensitivity to masting. For instance, species that are more sensitive to atmospheric nitrogen pollution (nitrophobic versus nitrotolerant) are thought to require more carbon from their tree hosts, although other possible explanations exist (Bidartondo et al., 2001; Lilleskov et al., 2019; Wallander, 1995). Additionally, ectomycorrhizal fungi with mycelial growth that extends further into the soil are thought to require more carbon and other nutrients (Agerer, 2001; Fernandez et al., 2017; Lilleskov et al., 2011). These differences may render species that are more resource-demanding more sensitive to potential resource limitation induced by mast seeding.

Studying fungal sporocarp production has been central to the field of fungal ecology for decades, especially as a proxy for fungal resource availability. While sporocarp production

is not a perfect proxy for fungal resource availability, fruitification ultimately represents carbon and nutrient investment in sexual reproduction, which fungi cannot do without the necessary resources (i.e., photosynthate and/or organic matter). Tree vegetative growth is linked to sporocarp production, both experimentally (C. Andrew & Lilleskov, 2009) and in observational studies (Collado et al., 2018; Egli et al., 2010), reifying our hypothesis that mast seeding and consequent resource switching in trees may reduce resource availability and fruitification by extension among forest dwelling fungi.

To evaluate the potential relationship between mast seeding in trees and fungal resource availability, we coupled two high-resolution, long-term ecological time series datasets: A) a fungal fruiting census spanning 1977–2006 from Payerne, Switzerland and B) a contemporaneous time series reconstruction of seed production in the dominant overstory tree species, European beech (*Fagus sylvatica* L.). We analyzed the data at three ecological scales: 1) total sporocarp production, 2) guild-level sporocarp production, and 3) species-level sporocarp production. We expected a negative relationship between beech seed production and sporocarp production and for ectomycorrhizal sporocarp production to be more negatively associated with seed production than saprotrophic sporocarp production. We tested whether 1) total sporocarp production, community composition, and diversity decreased with increasing beech seed production, and 2) if the relationship between sporocarp and beech seed production differed at the guild level between ectomycorrhizal and saprotrophic fungi. At the species level, we tested 3a) whether the proportion of species with significant relationships with masting differed between ectomycorrhizal and

saprotrophic fungi, 3b) if ectomycorrhizal species' sensitivity was explained by traits putatively corresponding to resource demand.

Materials and Methods

Site description

The fungal census was conducted in the 75-hectare La Chanéaz Fungal Reserve, established in 1975, near Payerne, Switzerland (Swiss Federal Institute for Forest, Snow and Landscape Research WSL; 46 degrees 47' 55" to 46 degrees 48' 10" N and 6 degrees 59' 52" to 7 degrees 00' 30" E (Straatsma et al., 2001). The site is an old-growth forest on the Swiss Central Plateau (mean altitude 585 m), dominated by multi-story beech (*Fagus sylvatica*), with interspersed spruce (*Picea abies*), larch (*Larix decidua*), oak (*Quercus robur*), pine (*Pinus sylvestris* and *Pinus strobus*), maple (*Acer pseudoplatanus*) and ash (*Fraxinus excelsior*) growing on calcareous cambisol. The study area was enclosed by 2-m fences to deter mushroom pickers and other large animals from harvesting the fruiting fungi.

From 1977–2006, a total of 106,521 epigeous sporocarps from fungi with macroscopic sporocarps were recorded and identified. Surveys were conducted on a weekly basis, during the May to November growing season, among five 300 m² plots. These plots were subdivided into three 100 m² subplots, each of which experienced a distinct mushroom surveying / harvesting procedure: picking, cutting, and no harvest (Egli et al., 2006). From the years 1980–1983, only edible species were recorded. Data from these years were

excluded from analyses of annual sporocarp production. Species taxonomies were updated by Andrew et al. (2016), and included synonymies and nomenclatural changes, based on Index Fungorum and Species Fungorum (<http://www.indexfungorum.org>; www.speciesfungorum.org). Further information on the mushroom sampling procedure is detailed in Straatsma et al. (2001) and Egli et al. (2006). Sporocarp counts and presence/absence data were both modelled in this current study, detailed in the statistical analyses section below (C. Andrew et al., 2016).

Beech masting record compilation

Beech seed production records were compiled from the MASTREE+ database (Hackett-Pain et al., 2022). The temporal dynamics of beech seed production show high synchrony within large portions of the species' range (Vacchiano et al., 2017), in which mast seed production is predicted by spring temperatures in the two years preceding the mast crop and is affected by long-term climate oscillations on decadal scales (Ascoli et al., 2017). We compiled all >5-year records of seed production within the 'southern region' identified by Vacchiano et al (2017) resulting in 80 unique time series of beech seed production (Appendix S3.2). These datasets were from Switzerland, Italy, and France. Records were constrained to those of beech seed or fruit production, such that records of pollen or flower abundance were dropped. In the region of our dataset, the frequency of mast years of beech has increased over the time period of the dataset, though to a lesser degree than in Great Britain (Bogdziewicz et al., 2020; Nussbaumer et al., 2016). To combine these datasets, we standardized each dataset to its range, resulting in a seed production score from 0-1 for

each year (e.g. Pearse *et al.* 2020). Or, where Ast is standardized annual seed production, A is one observation in a long-term seed production time series (SP):

$$Ast = (A - \min(SP)) / (\max(SP) - \min(SP))$$

We used the annual mean of datasets as the region-level index of mast seeding (Figure 3.1). The mast index was strongly positively correlated ($r=0.6$, $P<0.0001$) with the long-term (1986-2011) estimate of seed production nearest to the fungal study site, MASTREE record 3149, suggesting that the mast index accurately represents local seed production.

Meteorological record compilation

Historical daily precipitation and temperature data from 1977–2006 were compiled from the nearest weather station (Meteo Payerne, 7 km away; 46 degrees 48' 42" N, 6 degrees 56' 33" E; 490 m altitude) of the Federal Office of Meteorology and Climatology, MeteoSwiss (<http://www.meteoschweiz.admin>). Daily temperature and precipitation were averaged across the years and included in models of sporocarp production (Figure 3.1).

Species traits compilation

Fungal traits for all taxa were compiled from Knudsen and Vesterholt (2008) and Breitenbach and Kränzlin (1991, 1994, 2000, 2005). The following sporocarp traits were extracted from the texts: nutritional mode or guild (i.e., saprotroph or ectomycorrhizal). The FungalTraits database were also used to assign guild to species (Pölme *et al.*, 2020).

For ectomycorrhizal species ($n = 200$), extraradical mycelial exploration type was assigned at the genus level using literature sources (Agerer, 2006; Lilleskov et al., 2011; Tedersoo & Smith, 2013). Species with long-distance, medium-distance fringe, and medium-distance mat exploration types typically produce hydrophobic extraradical mycelium, and were designated hydrophobic, while those with contact, short-distance, and medium-distance smooth types were designated hydrophilic (Agerer, 2001; Unestam & Sun, 1995). Potential ectomycorrhizal fungal nitrophobicity was assigned to 24 species using literature sources (van Strien et al., 2018; van der Linde et al., 2018).

Data analyses

All analyses were performed in R (R Core Team, 2023). To evaluate the relationship between total sporocarp production and interannual variability in beech seed production, we calculated total annual sporocarp counts (115,417 sporocarps) and guild level annual sporocarp counts (54,583 ectomycorrhizal sporocarps, 38,811 saprotrophic sporocarps) across the fifteen subplots at La Chanéaz. Because records from 1980–1983 were incomplete, we excluded these data (93,329 remaining sporocarp observations). For models of total and guild-level annual sporocarp production, we constructed negative binomial regression models using the *glmmTMB* package (Brooks et al., 2017) and the *nbinom1* family parameterization. Our models included annual sporocarp counts as our response variable, with mean annual temperature, precipitation, and annual beech seed production index as fixed effects. Pairwise correlations between fixed effects were

examined prior to modeling, and showed no significant correlations, consistent with general observations that annual seed production and current-year weather are relatively decoupled (Appendix S3.1). For both models, plot and subplot were included as random effects, with subplot nested within plot to reflect the study site design. Residuals were simulated using DHARMA (Hartig & Lohse, 2022) and inspected for non-linearity, heteroscedasticity, and zero-inflation. For the analysis of total sporocarp production, residual non-linearity was detected; specifically, a hump-shaped relationship was detected between residuals and mean annual temperature. To address this, we introduced natural splines in our temperature predictor using the splines R base package (R Core Team, 2023) with two degrees of freedom. At the guild level, we included fixed intercept terms for guild and interactions between guild and seed production. We also included a dispersion formula with guild as the response variable to address varying dispersion between guilds. For both models, predicted sporocarp counts at different levels of seed production, mean temperature and precipitation were generated using the ggeffects package (Lüdtke, 2018). Partial residuals for visualization were generated using the “partialize” function in the jtools package (Long, 2023) and subset below the maximum observed counts to aid visualization.

We also examined relationships between beech seed production, current-year weather, and sporocarp community composition, diversity, and richness. We used the “capscale” function in the ape package (Paradis & Schliep, 2019) to perform a distance-based redundancy analysis (dbRDA) using the Bray-Curtis dissimilarity metric with mean annual

precipitation, mean annual temperature, and seed production as predictors (Paradis & Schliep, 2019). We performed an analysis of variance (ANOVA) on the overall model fit and the terms of the model with 999 permutations. We then calculated annual fungal species richness and diversity (Shannon-Weiner) at the plot level (to mitigate excessive zeros, $n = 5$ plots per year) and regressed these values against annual seed production, mean annual temperature, and mean annual precipitation with plot as a random effect. We modeled species richness with a negative binomial regression (“nbinom1” family in glmmTMB) and diversity with a gaussian distribution in glmmTMB (Brooks et al., 2017).

To evaluate species-level responses to seed production, temperature, and precipitation, we modeled annual sporocarp production for each species using logistic regression with mixed effects. For edible species whose occurrences were recorded from 1980-1983, we included data from these years. Using the package glmmTMB, we modeled presence-absence data (0, 1) based on beech seed production, mean annual temperature, and mean annual precipitation. Because sample sizes became limited at the species level, we scaled temperature and precipitation variables to enhance model convergence. Plot and subplot were included again as random effects, with subplot nested within plot. To capture species’ sensitivity to these environmental variables, we ran logistic regression models for each species sequentially, ordered by decreasing species’ frequency. We fit models to 250 species before species-level data became too sparse to fit models. We extracted z scores associated with each predictor for each species. The z score is the statistic associated with the likelihood of observing the estimated coefficient given the variability in the input data

and the null hypothesis. Given an alpha level of 0.05, if the absolute value of the z score is greater than 1.96, the likelihood of observing the estimated coefficient is sufficiently low (below 0.05) to reject the null hypothesis that there is no relationship between the response variable and the predictor. In context, a sufficiently low z score associated with beech seed production indicates that there is evidence that a species is less likely to be observed at high levels of seed production, i.e., a mast year. This analysis yielded z scores associated with 151 species of ectomycorrhizal fungi and 96 species of saprotrophic fungi. Fisher's exact tests were used to test whether the proportions of species associated with beech seed production versus unassociated varied across guilds. Among ectomycorrhizal fungi, this test was performed to detect whether the proportion of species significantly associated with seed production varied by ectomycorrhizal exploration type, mycelial hydrophobicity, and potential nitrophobicity.

Results

Total sporocarp production was strongly negatively related to beech seed production (coefficient \pm standard error: -1.15 ± 0.20 log(sporocarp count) per unit seed production, $z = -5.660$, $p < 0.001$) (Figure 3.2a). Conversely, sporocarp production was positively related to temperature and precipitation (temperature, first spline: 2.18 ± 0.28 log(sporocarp count) $^{\circ}\text{C}^{-1}$, $z = 7.811$, $p < 0.001$; temperature, second spline: 0.42 ± 0.15 log(sporocarp count) $^{\circ}\text{C}^{-1}$, $z = 2.845$, $p < 0.01$; precipitation: 0.57 ± 0.15 log(sporocarp count) mm^{-1} , $z = 5.882$, $p < 0.001$). Total sporocarp counts declined by an average of 55% based on seed production, from an average of 406 sporocarps at lowest seed production (95% CI: 305.97–539.36 per

100 m² yr⁻¹) to an average of 183 sporocarps at highest seed production (95% CI: 140.47–238.47 per 100 m² yr⁻¹), at mean levels of temperature and precipitation. The composition of the total sporocarp community was also significantly related to mean annual temperature ($F = 5.497$, $p = 0.001$), mean annual precipitation ($F = 3.340$, $p = 0.001$), and beech seed production ($F = 2.279$, $p = 0.002$) (dbRDA, $F = 3.705$, $p = 0.001$) (Figure 3.3). Mean annual precipitation and seed production were oppositely related to community composition (Figure 3.3). Species richness was negatively associated with seed production (-0.59 ± 0.23 log(species) per unit seed production, $z = -2.569$, $p = 0.010$), and positively associated with mean annual temperature (0.40 ± 0.06 log(species) °C⁻¹, $z = 6.265$, $p < 0.001$) and mean annual precipitation (0.31 ± 0.11 log(species) mm⁻¹, $z = 2.623$, $p = 0.009$). Specifically, from the lowest to highest level of seed production, species richness declined 34% on average, from 39 species (28.26–53.06 per 100 m² yr⁻¹) to 26 species (18.69–35.27 per 100 m² yr⁻¹). Shannon-Weiner diversity was also negatively associated with seed production (-0.57 ± 0.24 per unit seed production, $z = -2.331$, $p = 0.022$), positively related to temperature (0.35 ± 0.07 °C⁻¹, $z = 4.731$, $p < 0.001$) and positively related to precipitation (0.27 ± 0.13 mm⁻¹, $z = 2.035$, $p = 0.042$ mm⁻¹) (Appendix S3.3).

At the guild level, sporocarp production was negatively associated with seed production among both ectomycorrhizal and saprotrophic fungi (ectomycorrhizal: -1.01 ± 0.22 log(sporocarp count) per unit seed production, $z = -4.625$, $p < 0.001$; saprotrophic: -0.69 ± 0.22 log(sporocarp count) per unit seed production, $z = -3.18$, $p = 0.001$). The relationship between seed production and sporocarp production trended more negative for

ectomycorrhizal fungi, compared to saprotrophic fungi, although this was not significant (-0.31 ± 0.30 log(sporocarp count) per unit seed production, $z = -1.041$, $p = 0.298$). Ectomycorrhizal sporocarp counts declined by 50%, on average, from 193 sporocarps (95% CI: 193.11–96.16 per 100 m² yr⁻¹) with lowest seed production to 96 sporocarps per 100 m² yr⁻¹ (95% CI: 72.50–127.54 per 100 m² yr⁻¹) with greatest seed production, at mean temperature and precipitation. Saprotrophic sporocarp production declined by 38%, on average, from 123 sporocarps per 100 m² yr⁻¹ (95% CI: 93.39–163.13 per 100 m² yr⁻¹) with lowest seed production to 76.42 sporocarps per 100 m² yr⁻¹ (95% CI: 57.60–101.38 per 100 m² yr⁻¹) at highest seed production (Figure 3.2b).

At the species level, out of the 280 ectomycorrhizal and saprotrophic species that fruited adequately to fit models, 27 species (10%) were significantly less likely to produce fruitbodies as beech seed production increased (z score < -1.96) (Figure 3.4). These species produced 29% of all the fruitbodies recorded at the fungal reserve ($n = 30918$). One terrestrial saprotrophic fungal species (*Gymnopus ocior*) was more likely to be observed as beech seed production increased (z score > 1.96 , $n = 189$) (Table 3.1). Across guilds, however, there were no significant differences in the proportion of species with significant associations with beech seed production (Fisher's exact test, $p = 0.786$): 15/172 (9%) of ectomycorrhizal fungal species and 12/108 (11%) of saprotrophic fungal species were significantly less likely to produce fruitbodies during a mast seeding event (Figure 3.4). The top 25 most abundant species and information about their relationship with beech seed production is presented in Table 3.1. Among ectomycorrhizal fungi, neither potential

nitrophobicity, mycelial hydrophobicity, nor extraradical mycelial exploration type explained species' fruiting response to masting (Fisher's exact test, $p = 0.32$; $p = 0.88$, $p = 0.96$).

Discussion

Our findings suggest that both the magnitude of fungal sporocarp production and sporocarp community composition is tightly linked to interannual variability in overstory tree seed production. Specifically, the highest level of annual seed production in European beech was associated with a 55% reduction in total fungal sporocarp production. High seed production in beech was also associated with reduced fungal sporocarp species richness and diversity as well as shifts in community composition. Together, this pattern is consistent with the hypothesis that tree investment in a mast seed crop decreases resource availability to fungi, limiting fungal reproductive investment. Although the magnitude of ectomycorrhizal sporocarp production was marginally more negatively related to seed production than in saprotrophic fungi, both guilds showed reduced fruiting in mast years. This finding suggests that the relationship between interannual variability in seed production and fungi extends beyond the ectomycorrhizal fungal community, highlighting the dependence multiple guilds of soil fungi on trees (Koide et al., 2014). Indeed, similar proportions of ectomycorrhizal and saprotrophic fungal species had significant relationships with seed production.

Our findings are consistent with the causal hypothesis that mast seeding temporarily depletes tree and soil resources, resulting in reduced fungal fruiting. However, as an observational study, it is important to consider alternate explanations of the negative correlation between annual seed production and fungal fruiting. First, it could be imagined that both fungal fruiting and seed production could respond to the same set of environmental drivers (environmental covariation). In beech, however, this is unlikely because beech seed crops are strongly predicted by high temperature in July in the year preceding seed production (Y-1) and low July temperatures in the year preceding that (Y-2) (Bogdziewicz et al., 2023). Temperature at these lagged time periods has not been shown to affect fungal sporocarp production, which is more strongly associated with recent weather conditions (Sato et al., 2012). Collado et al. (2018) did find that saprotrophic sporocarp production was linked to tree growth two years previous, however, suggesting that lagged environmental conditions may play a role in fungal fruiting. However, the direct role of lag effects to fruiting-year carbon availability, versus instead indirect effects to other aspects relating to fungal biology (e.g., root dynamics, compositional interactions, spore germination or vegetative growth) that then impact future fruiting, remains, at this point, unexplored. Second, it may be possible that high fungal sporocarp production could inhibit masting in non-mast years (reversed causation). Again, this is unlikely because beech mast events are largely determined by the number of flower primordia produced, an event that happens over a year prior to the seed crop and fungal fruiting event (Gruber, 2003). It is possible that high fungal biomass or production, indicated by high sporocarp production, could limit plant nutrient availability and thereby primordia production through nutrient

immobilization (Näsholm et al., 2013; Tanentzap et al., 2012), but we did not find a relationship between seed production the year previous and fungal fruiting (data not shown). Finally, we note that seed production data was inferred from many historical records instead of measured at the site. This introduces uncertainty in our analysis, since masting behavior at the site may have differed somewhat from the record we assembled. We stress, however, that masting is by definition synchronous, and at large geographic scales (Koenig & Knops, 1998; Vacchiano et al., 2017). Taken together, although the results support our causal hypothesis, we maintain that these findings are correlative and require further investigation.

Analysis of fungal sporocarp community composition revealed that mean annual precipitation and seed production were oppositely related to community composition (Figure 3.3). This suggests that fungal community composition during a dry year resembled that during a year of high seed production. During a drought year, microbial activity is stymied by reduced water availability (Schimel, 2018). Our finding could indicate that high seed production necessitates greater water uptake from soil, resembling droughted conditions. The effects of mast seeding on soil conditions and processes, however, has rarely been studied (Zackrisson et al., 1999), rendering this supposition speculative. To further interrogate links among soil resource availability, masting, and fungal community composition, we encourage long-term monitoring of soil moisture and nutrient availability in forests where masting is also recorded. This monitoring is particularly important in the context of shifting climatic conditions, which have already been shown to negatively affect

the magnitude of masting in European beech forests (Bogdziewicz et al., 2020, 2023). If, for example, masting frequency decreases, but the same forests experience more frequent droughts, it seems likely that the inter-annual community shifts we observed here may be a harbinger of future fungal sporocarp composition in European beech forests.

Among ectomycorrhizal fungi, we evaluated whether differences in fungal traits putatively associated with resource demand explained whether species showed significant relationships with seed production. Previously, ectomycorrhizal species with prolific, highly ramified, and hydrophobic exploratory mycelia have been assumed to be more costly to their hosts, because they purportedly require more carbon and nutrients to sustain vegetative tissue production (Karst et al., 2021; Lilleskov et al., 2011). This logic has been used to explain why many fungal species with these convergent traits are sensitive to nitrogen deposition (Lilleskov et al., 2011); nitrogen deposition is assumed to decrease photosynthate availability to ectomycorrhizal fungi and, hence, limit those that require substantial carbon. This explanation, in turn, has reified a link between species' nitrophobicity and carbon cost (Lilleskov et al., 2019). Here, we found evidence that mast seeding may reduce resource availability to ectomycorrhizal fungi, as evidenced by decreased sporocarp production. Yet, the mycelial traits associated with high resource demand did not explain the species-level relationships with mast seeding. For example, similar proportions of species showed significant relationships with seed production across extraradical mycelial exploration types, groups with hydrophobic versus hydrophilic extraradical mycelia, and putative nitrophobicity. Among the 15 ectomycorrhizal species

significantly negatively associated with seed production (Table 3.1), both species with hydrophobic and hydrophilic exploratory hyphae were present. Additionally, among the taxa with significant associations with beech seed production was *Russula ochroleuca*, a putatively nitrotolerant species (van Strien et al., 2018; van der Linde et al., 2018) (Table 3.1). These findings suggest that current traits that have been previously linked to resource demand in ectomycorrhizal fungi are not sufficient to describe species' sensitivity to resource scarcity across more diverse situations of carbon availability (Bidartondo et al., 2001; Jörgensen et al., 2023; Wallander, 1995).

Our findings open a novel line of research at the intersection of mast seeding and fungal ecology. In general, we speculate that masting may have wide-ranging effects on soil processes, though these have only rarely been explored (Zackrisson et al., 1999). These hypotheses could be tested by monitoring soil moisture levels, rates of nutrient cycling, and hyphal production and turnover during mast and non-mast years or by experimentally altering mast crops or root connections within the soil. Similarly, it would be useful to explore the geographic, taxonomic, and environmental scope of the connection between masting and fungal fruiting. This effort will be aided by widespread records of long-term seed production (e.g. Hacket-Pain et al., 2022) and comparable multi-decadal sporocarp surveys (e.g. Bonet et al., 2012; Sato et al., 2012; van Strien et al., 2018). Additionally, we suggest that quantification of sporocarp production by other fungal guilds may also reveal important insights about the scope of masting effects. For example, we hypothesize that fungi that are pathogens on living trees, such as the 'humongous fungus', *Armillaria*

mellea, may also experience significant decreases in sporocarp production in mast years, while fungi living on dead trees, i.e. wood decay fungi, may have no relationship with masting-related resource shifts. Finally, assessing how masting is related to the size, biomass, and stoichiometry of sporocarps would further clarify how changes in resource availability impact fungal fructification (Hobbie et al., 2021). Answering this latter question might be possible using careful measures of herbarium specimens (C. Andrew et al., 2019), which provide an underappreciated resource for studies of fungal responses to altered environmental conditions.

Conclusions

This study is the first to evaluate the potential linkage between mast seeding and fungal sporocarp production. We have demonstrated a strong inverse relationship between beech seed production and fungal sporocarp production, diversity, and species richness. We have also shown that ectomycorrhizal and saprotrophic fungi show comparable declines in fruitification with increasing beech seed production, despite key differences in their ecology. Mast seeding has been linked to the abundance and feeding habits of numerous animals that consume seeds or have trophic links to those that do (e.g. Ostfeld *et al.* 2000; Stephens *et al.* 2019), resulting in a ‘rhythm’ to many aboveground forest processes (Pesendorfer et al., 2021). Our findings suggest that this ‘rhythm’ extends belowground, amplifying the ecological significance of masting. This rhythm may be disrupted as climate change alters the frequency and magnitude of masting (Bogdziewicz et al., 2020, 2023). The results of our study also suggest that masting may create a broad ‘pull’ on soil

resources that significantly alters resource availability for fungal (and likely other microbial) guilds. Indeed, the composition of the sporocarp community during a mast year resembled that during droughted conditions. Whether this pattern emerges across diverse forests remains unknown, as do the proximal mechanisms driving decreased sporocarp production. We argue that mast seeding may be an underappreciated driver of fungal activity and call for further research.

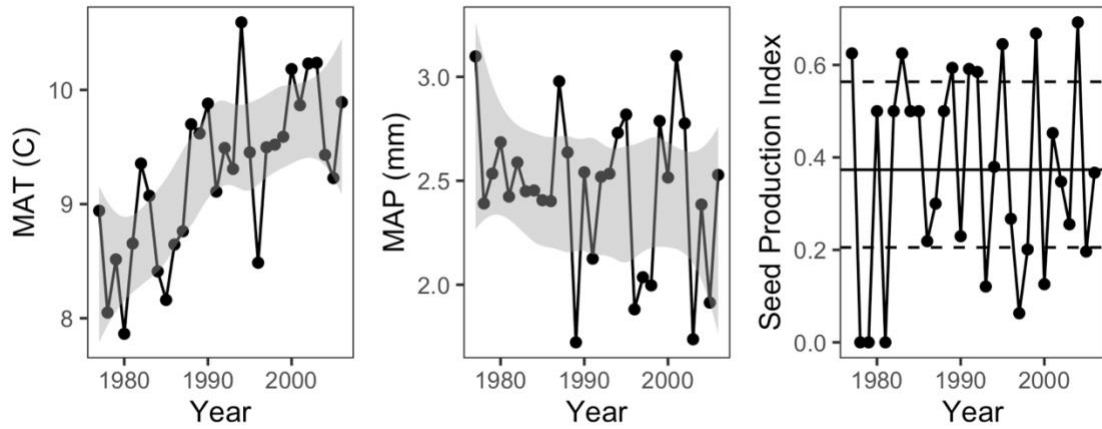


Figure 3.1. Climate (panels one and two) and beech seed production (third panel) data from 1977–2006 for Payerne, Switzerland. For mean annual temperature (MAT) and mean annual precipitation (MAP), the shaded region represents the 95% confidence interval around a loess curve fit to the data. For beech seed production, each point represents an annual index of beech seed production derived from MASTREE+. Dotted lines represent the interquartile range of the data.

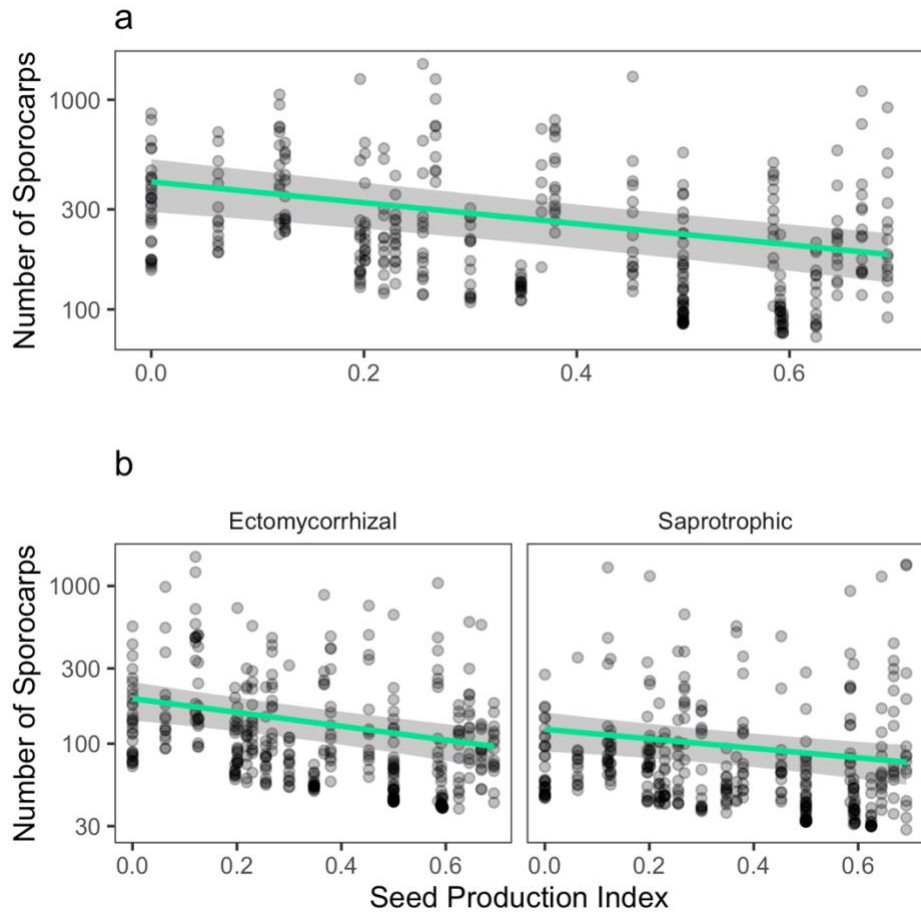


Figure 3.2. Relationship between beech seed production and a) total fungal sporocarp production, and b) guild-level sporocarp production from 1977–2006. Points represent residual variation in sporocarp production after accounting for variation arising from mean annual precipitation and mean annual temperature. The green line represents the mean line estimated for the relationship between beech seed production and sporocarp production predicted via negative binomial multiple regression. The shaded intervals represent 95% confidence intervals around the mean lines.

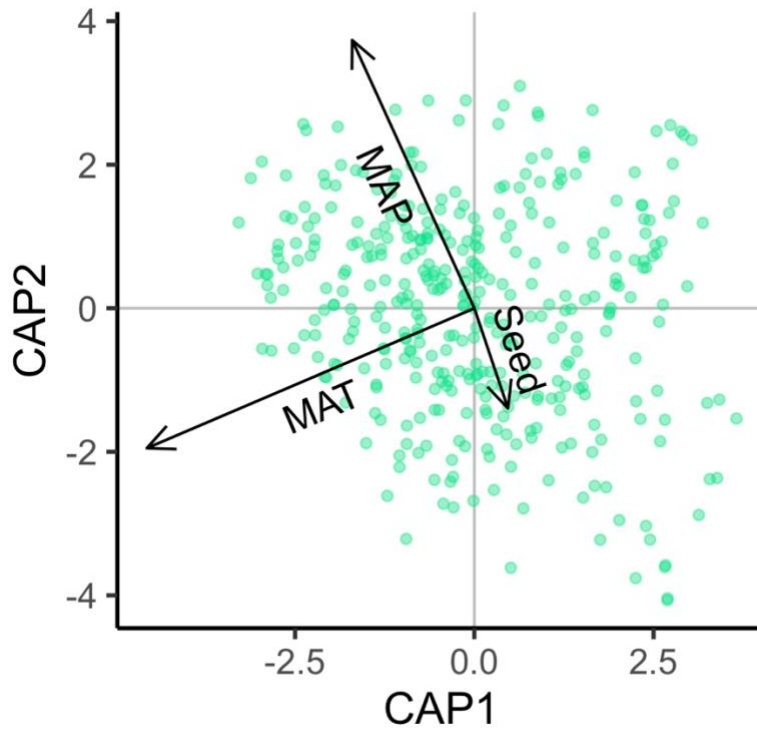


Figure 3.3. Distance-based redundancy analysis showing the relationships between fungal sporocarp community composition and mean annual precipitation (MAP), mean annual temperature (MAT), and beech seed production (Seed).

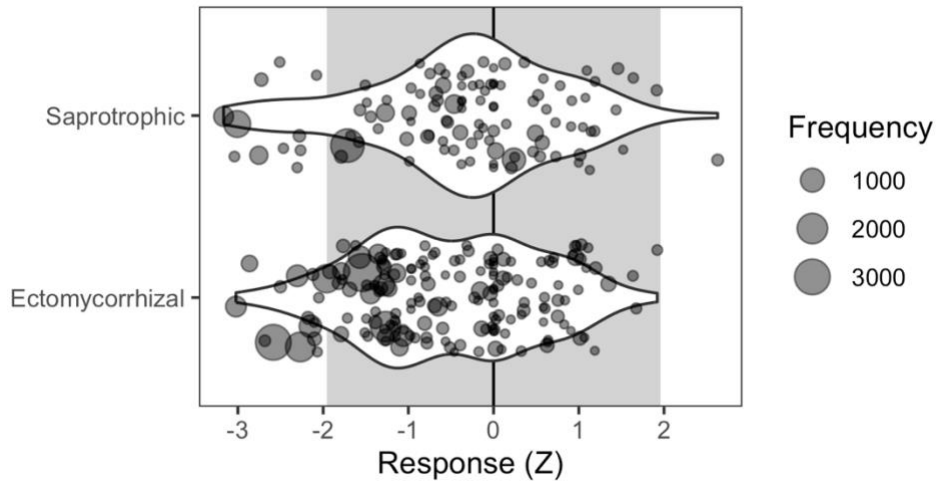


Figure 3.4. Variation in fungal species' relationships with beech seed production derived from multiple logistic regression models. Each point represents the z score associated with the modelled relationship between one species' presence and beech seed production from 1977–2006. The shaded interval shows the range of non-significant z scores using an alpha level of 0.05 (cutoffs: -1.96, 1.96). Point size corresponds to the total number of presences, or the frequency of observation for a species.

Table 3.1. Top 25 most abundant fungal species observed at La Chanéaz, with reference to their total abundance (Total Fruitbodies), ecological guild (Guild), whether they showed a significant association with European beech seed production (Association: Seed Production), their habitat (Habitat, broadleaf and/or conifer). For ectomycorrhizal fungi, exploration type and association with atmospheric nitrogen deposition (nitrophobicity) if known is included.

Species	Total Fruitbodies	Guild	Association: Seed Production	Habitat	Exploration Type	Nitrophobicity
<i>Cortinarius caperatus</i>	3399	Ectomycorrhizal	Not	Broadleaf/Conifer	Medium-distance fringe	Nitrophobic
<i>Cortinarius flexipes</i>	1767	Ectomycorrhizal	Not	Broadleaf/Conifer	Medium-distance fringe	
<i>Craterellus cornucopioides</i>	8634	Ectomycorrhizal	Negative	Broadleaf	Short-distance delicate	
<i>Craterellus tubaeformis</i>	1702	Ectomycorrhizal	Not	Conifer	Short-distance delicate	Nitrophobic
<i>Hygrophorus eburneus</i>	1759	Ectomycorrhizal	Negative	Broadleaf	Contact	
<i>Inocybe petiginosa</i>	1003	Ectomycorrhizal	Not	Broadleaf	Short-distance delicate	
<i>Laccaria amethystina</i>	12073	Ectomycorrhizal	Not	Broadleaf/Conifer	Short-distance delicate	
<i>Laccaria laccata</i>	1627	Ectomycorrhizal	Not	Broadleaf/Conifer	Short-distance delicate	Tolerant
<i>Lactarius blennius</i>	2846	Ectomycorrhizal	Negative	Broadleaf	Medium-distance smooth	
<i>Russula cyanoxantha</i>	935	Ectomycorrhizal	Not	Broadleaf/Conifer	Contact	Tolerant
<i>Russula fellea</i>	1330	Ectomycorrhizal	Negative	Broadleaf	Contact	
<i>Russula nobilis</i>	2848	Ectomycorrhizal	Not	Broadleaf	Contact	
<i>Russula ochroleuca</i>	5530	Ectomycorrhizal	Negative	Broadleaf/Conifer	Contact	Tolerant
<i>Xerocomellus chrysenteron</i>	2475	Ectomycorrhizal	Negative	Broadleaf/Conifer	Long-distance	
<i>Clitocybe gibba</i>	1859	Saprotrophic	Not	Broadleaf/Conifer		
<i>Entoloma rhodopolium</i>	927	Saprotrophic	Not	Broadleaf	Medium-distance smooth	
<i>Gymnopus confluens</i>	1115	Saprotrophic	Not	Broadleaf/Conifer		
<i>Gymnopus dryophilus</i>	1641	Saprotrophic	Negative	Broadleaf/Conifer		
<i>Hypholoma fasciculare</i>	7209	Saprotrophic	Not	Broadleaf/Conifer		
<i>Kuehneromyces mutabilis</i>	6946	Saprotrophic	Not	Broadleaf/Conifer		
<i>Mycena galopus</i>	1353	Saprotrophic	Negative	Broadleaf/Conifer		
<i>Mycena pura</i>	3154	Saprotrophic	Negative	Broadleaf/Conifer		
<i>Pholiota squarrosa</i>	848	Saprotrophic	Not	Broadleaf/Conifer		
<i>Rhodocollybia butyracea</i>	6242	Saprotrophic	Not	Conifer		

Bibliography

- Agerer, R. (2001). Exploration types of ectomycorrhizae. *Mycorrhiza*, 11(2), 107–114. <https://doi.org/10.1007/s005720100108>
- Agerer, R. (2006). Fungal relationships and structural identity of their ectomycorrhizae. *Mycological Progress*, 5(2), 67–107. <https://doi.org/10.1007/s11557-006-0505-x>
- Alberton, O., Kuyper, T. W., & Gorissen, A. (2007). Competition for nitrogen between *Pinus sylvestris* and ectomycorrhizal fungi generates potential for negative feedback under elevated CO₂. *Plant and Soil*, 296(1), 159. <https://doi.org/10.1007/s11104-007-9306-5>
- Andrew, C., Diez, J., James, T. Y., & Kausserud, H. (2019). Fungarium specimens: A largely untapped source in global change biology and beyond. *Philosophical Transactions of the Royal Society B: Biological Sciences*, 374(1763), 20170392. <https://doi.org/10.1098/rstb.2017.0392>
- Andrew, C., Heegaard, E., Halvorsen, R., Martinez-Peña, F., Egli, S., Kirk, P. M., Bässler, C., Büntgen, U., Aldea, J., Høiland, K., Boddy, L., & Kausserud, H. (2016). Climate impacts on fungal community and trait dynamics. *Fungal Ecology*, 22, 17–25. <https://doi.org/10.1016/j.funeco.2016.03.005>
- Andrew, C., & Lilleskov, E. A. (2009). Productivity and community structure of ectomycorrhizal fungal sporocarps under increased atmospheric CO₂ and O₃. *Ecology Letters*, 12(8), 813–822. <https://doi.org/10.1111/j.1461-0248.2009.01334.x>
- Andrew, R. M., & Peters, G. P. (2023). *The Global Carbon Project's fossil CO₂ emissions dataset* (Version 2023v36) [dataset]. Zenodo. <https://doi.org/10.5281/zenodo.10177738>
- Arneith, A., Lloyd, J., Šantrůčková, H., Bird, M., Grigoryev, S., Kalaschnikov, Y. N., Gleixner, G., & Schulze, E.-D. (2002). Response of central Siberian Scots pine to soil water deficit and long-term trends in atmospheric CO₂ concentration. *Global Biogeochemical Cycles*, 16(1), 5-1-5–13. <https://doi.org/10.1029/2000GB001374>
- Arnolds, E. (1991). Decline of ectomycorrhizal fungi in Europe. *Agriculture, Ecosystems & Environment*, 35(2), 209–244. [https://doi.org/10.1016/0167-8809\(91\)90052-Y](https://doi.org/10.1016/0167-8809(91)90052-Y)
- Ascoli, D., Vacchiano, G., Turco, M., Conedera, M., Drobyshev, I., Maringer, J., Motta, R., & Hacket-Pain, A. (2017). Inter-annual and decadal changes in teleconnections drive continental-scale synchronization of tree reproduction. *Nature Communications*, 8(1), Article 1. <https://doi.org/10.1038/s41467-017-02348-9>
- Averill, C., Dietze, M. C., & Bhatnagar, J. M. (2018). Continental-scale nitrogen pollution is shifting forest mycorrhizal associations and soil carbon stocks. *Global Change Biology*, 24(10), 4544–4553. <https://doi.org/10.1111/gcb.14368>
- Bailey, R. G. (2014). *Ecoregions: The Ecosystem Geography of the Oceans and Continents*. Springer New York. <https://doi.org/10.1007/978-1-4939-0524-9>
- Baldrian, P. (2008). Chapter 2 Enzymes of saprotrophic basidiomycetes. In *British Mycological Society Symposia Series* (Vol. 28, pp. 19–41). Elsevier. [https://doi.org/10.1016/S0275-0287\(08\)80004-5](https://doi.org/10.1016/S0275-0287(08)80004-5)

- Baldrian, P., López-Mondéjar, R., & Kohout, P. (2023). Forest microbiome and global change. *Nature Reviews Microbiology*, 1–15. <https://doi.org/10.1038/s41579-023-00876-4>
- Barceló, M., van Bodegom, P. M., & Soudzilovskaia, N. A. (2023). Fine-resolution global maps of root biomass carbon colonized by arbuscular and ectomycorrhizal fungi. *Scientific Data*, 10(1), Article 1. <https://doi.org/10.1038/s41597-022-01913-2>
- Bassett, K. R., Östlund, L., Gundale, M. J., Fridman, J., & Jämtgård, S. (2023). Forest inventory tree core archive reveals changes in boreal wood traits over seven decades. *Science of The Total Environment*, 900, 165795. <https://doi.org/10.1016/j.scitotenv.2023.165795>
- Bates, D., Mächler, M., Bolker, B., & Walker, S. (2015). Fitting Linear Mixed-Effects Models Using lme4. *Journal of Statistical Software*, 67, 1–48. <https://doi.org/10.18637/jss.v067.i01>
- Belmecheri, S., & Lavergne, A. (2020). Compiled records of atmospheric CO2 concentrations and stable carbon isotopes to reconstruct climate and derive plant ecophysiological indices from tree rings. *Dendrochronologia*, 63, 125748. <https://doi.org/10.1016/j.dendro.2020.125748>
- Bessette, A. E., Bessette, A. R., & Fischer, D. W. (1997). *Mushrooms of Northeastern North America*. Syracuse University Press.
- Bidartondo, M. I., Ek, H., Wallander, H., & Söderström, B. (2001). Do nutrient additions alter carbon sink strength of ectomycorrhizal fungi? *New Phytologist*, 151(2), 543–550. <https://doi.org/10.1046/j.1469-8137.2001.00180.x>
- Bogdziewicz, M., Journé, V., Hacket-Pain, A., & Szymkowiak, J. (2023). Mechanisms driving interspecific variation in regional synchrony of trees reproduction. *Ecology Letters*, 26(5), 754–764. <https://doi.org/10.1111/ele.14187>
- Bogdziewicz, M., Kelly, D., Thomas, P. A., Lagueard, J. G. A., & Hacket-Pain, A. (2020). Climate warming disrupts mast seeding and its fitness benefits in European beech. *Nature Plants*, 6(2), Article 2. <https://doi.org/10.1038/s41477-020-0592-8>
- Bogdziewicz, M., Zwolak, R., & Crone, E. E. (2016). How do vertebrates respond to mast seeding? *Oikos*, 125(3), 300–307. <https://doi.org/10.1111/oik.03012>
- Bonet, J. A., de-Miguel, S., Martínez de Aragón, J., Pukkala, T., & Palahí, M. (2012). Immediate effect of thinning on the yield of *Lactarius deliciosus* in *Pinus pinaster* forests in Northeastern Spain. *Forest Ecology and Management*, 265, 211–217. <https://doi.org/10.1016/j.foreco.2011.10.039>
- Breitenbach, J., & Kränzlin, F. (1991). *Fungi of Switzerland, Volume 3: Boletes and Agarics, Part 1* (Vol. 3). Verlag Mykologia.
- Breitenbach, J., & Kränzlin, F. (1994). *Fungi of Switzerland, Volume 4: Agarics, Part 2* (Vol. 4). Verlag Mykologia.
- Breitenbach, J., & Kränzlin, F. (2000). *Fungi of Switzerland, Volume 5: Agarics, Part 3* (Vol. 5). Verlag Mykologia.
- Breitenbach, J., & Kränzlin, F. (2005). *Fungi of Switzerland, Volume 6: Russulaceae* (Vol. 6). Verlag Mykologia.
- Brooks, M., E., Kristensen, K., Benthem, K., J., van, Magnusson, A., Berg, C., W., Nielsen, A., Skaug, H., J., Mächler, M., & Bolker, B., M. (2017). glmmTMB Balances

- Speed and Flexibility Among Packages for Zero-inflated Generalized Linear Mixed Modeling. *The R Journal*, 9(2), 378. <https://doi.org/10.32614/RJ-2017-066>
- Chen, J., Hofmockel, K. S., & Hobbie, E. A. (2016). Isotopic Analysis of Sporocarp Protein and Structural Material Improves Resolution of Fungal Carbon Sources. *Frontiers in Microbiology*, 7. <https://doi.org/10.3389/fmicb.2016.01994>
- Clark, C. M., Phelan, J., Doraiswamy, P., Buckley, J., Cajka, J. C., Dennis, R. L., Lynch, J., Nolte, C. G., & Spero, T. L. (2018). Atmospheric deposition and exceedances of critical loads from 1800–2025 for the conterminous United States. *Ecological Applications*, 28(4), 978–1002. <https://doi.org/10.1002/eap.1703>
- Collado, E., Camarero, J. J., Martínez de Aragón, J., Pemán, J., Bonet, J. A., & de-Miguel, S. (2018). Linking fungal dynamics, tree growth and forest management in a Mediterranean pine ecosystem. *Forest Ecology and Management*, 422, 223–232. <https://doi.org/10.1016/j.foreco.2018.04.025>
- Craine, J. M., Brookshire, E. N. J., Cramer, M. D., Hasselquist, N. J., Koba, K., Marin-Spiotta, E., & Wang, L. (2015). Ecological interpretations of nitrogen isotope ratios of terrestrial plants and soils. *Plant and Soil*, 396(1), 1–26. <https://doi.org/10.1007/s11104-015-2542-1>
- Craine, J. M., Elmore, A. J., Aidar, M. P. M., Bustamante, M., Dawson, T. E., Hobbie, E. A., Kahmen, A., Mack, M. C., McLauchlan, K. K., Michelsen, A., Nardoto, G. B., Pardo, L. H., Peñuelas, J., Reich, P. B., Schuur, E. A. G., Stock, W. D., Templer, P. H., Virginia, R. A., Welker, J. M., & Wright, I. J. (2009). Global patterns of foliar nitrogen isotopes and their relationships with climate, mycorrhizal fungi, foliar nutrient concentrations, and nitrogen availability. *New Phytologist*, 183(4), 980–992. <https://doi.org/10.1111/j.1469-8137.2009.02917.x>
- Craine, J. M., Elmore, A. J., Wang, L., Aranibar, J., Bauters, M., Boeckx, P., Crowley, B. E., Dawes, M. A., Delzon, S., Fajardo, A., Fang, Y., Fujiyoshi, L., Gray, A., Guerrieri, R., Gundale, M. J., Hawke, D. J., Hietz, P., Jonard, M., Kearsley, E., ... Zmudczyńska-Skarbek, K. (2018). Isotopic evidence for oligotrophication of terrestrial ecosystems. *Nature Ecology & Evolution*, 2(11), Article 11. <https://doi.org/10.1038/s41559-018-0694-0>
- Craine, J. M., Elmore, A. J., Wang, L., Aranibar, J., Bauters, M., Boeckx, P., Crowley, B. E., Dawes, M. A., Delzon, S., Fajardo, A., Fang, Y., Fujiyoshi, L., Gray, A., Guerrieri, R., Gundale, M. J., Hawke, D. J., Hietz, P., Jonard, M., Kearsley, E., ... Zmudczyńska-Skarbek, K. (2019). *Data from: Isotopic evidence for oligotrophication of terrestrial ecosystems* (Version 1, p. 6505354 bytes) [dataset]. Dryad. <https://doi.org/10.5061/DRYAD.V2K2607>
- Crowther, T. W., Todd-Brown, K. E. O., Rowe, C. W., Wieder, W. R., Carey, J. C., Machmuller, M. B., Snoek, B. L., Fang, S., Zhou, G., Allison, S. D., Blair, J. M., Bridgham, S. D., Burton, A. J., Carrillo, Y., Reich, P. B., Clark, J. S., Classen, A. T., Dijkstra, F. A., Elberling, B., ... Bradford, M. A. (2016). Quantifying global soil carbon losses in response to warming. *Nature*, 540(7631), Article 7631. <https://doi.org/10.1038/nature20150>

- Dijkstra, F., Carrillo, Y., Pendall, E., & Morgan, J. (2013). Rhizosphere priming: A nutrient perspective. *Frontiers in Microbiology*, 4. <https://www.frontiersin.org/articles/10.3389/fmicb.2013.00216>
- Dong, Y., Wang, Z., Sun, H., Yang, W., & Xu, H. (2018). The Response Patterns of Arbuscular Mycorrhizal and Ectomycorrhizal Symbionts Under Elevated CO₂: A Meta-Analysis. *Frontiers in Microbiology*, 9. <https://doi.org/10.3389/fmicb.2018.01248>
- Egli, S., Ayer, F., Peter, M., Eilmann, B., & Rigling, A. (2010). Is forest mushroom productivity driven by tree growth? Results from a thinning experiment. *Annals of Forest Science*, 67(5), 509–509. <https://doi.org/10.1051/forest/2010011>
- Egli, S., Peter, M., Buser, C., Stahel, W., & Ayer, F. (2006). Mushroom picking does not impair future harvests – results of a long-term study in Switzerland. *Biological Conservation*, 129(2), 271–276. <https://doi.org/10.1016/j.biocon.2005.10.042>
- Elmore, A. J., Nelson, D. M., & Craine, J. M. (2016). Earlier springs are causing reduced nitrogen availability in North American eastern deciduous forests. *Nature Plants*, 2(10), Article 10. <https://doi.org/10.1038/nplants.2016.133>
- Fernandez, C. W., & Kennedy, P. G. (2016). Revisiting the ‘Gadgil effect’: Do interguild fungal interactions control carbon cycling in forest soils? *New Phytologist*, 209(4), 1382–1394. <https://doi.org/10.1111/nph.13648>
- Fernandez, C. W., Nguyen, N. H., Stefanski, A., Han, Y., Hobbie, S. E., Montgomery, R. A., Reich, P. B., & Kennedy, P. G. (2017). Ectomycorrhizal fungal response to warming is linked to poor host performance at the boreal-temperate ecotone. *Global Change Biology*, 23(4), 1598–1609. <https://doi.org/10.1111/gcb.13510>
- Fernandez, C. W., See, C. R., & Kennedy, P. G. (2019). Decelerated carbon cycling by ectomycorrhizal fungi is controlled by substrate quality and community composition. *bioRxiv*, 716555. <https://doi.org/10.1101/716555>
- Fox, J., & Weisberg, S. (2018). *An R Companion to Applied Regression*. SAGE Publications.
- Frey, S. D. (2019). Mycorrhizal Fungi as Mediators of Soil Organic Matter Dynamics. *Annual Review of Ecology, Evolution, and Systematics*, 50(1), 237–259. <https://doi.org/10.1146/annurev-ecolsys-110617-062331>
- Gadgil, R. L., & Gadgil, P. D. (1971). Mycorrhiza and Litter Decomposition. *Nature*, 233(5315), 133–133. <https://doi.org/10.1038/233133a0>
- Galloway, J. N., Dentener, F. J., Capone, D. G., Boyer, E. W., Howarth, R. W., Seitzinger, S. P., Asner, G. P., Cleveland, C. C., Green, P. A., Holland, E. A., Karl, D. M., Michaels, A. F., Porter, J. H., Townsend, A. R., & Vöosmarty, C. J. (2004). Nitrogen Cycles: Past, Present, and Future. *Biogeochemistry*, 70(2), 153–226. <https://doi.org/10.1007/s10533-004-0370-0>
- Gaudinski, J. B., Torn, M. S., Riley, W. J., Swanston, C., Trumbore, S. E., Joslin, J. D., Majdi, H., Dawson, T. E., & Hanson, P. J. (2009). Use of stored carbon reserves in growth of temperate tree roots and leaf buds: Analyses using radiocarbon measurements and modeling. *Global Change Biology*, 15(4), 992–1014. <https://doi.org/10.1111/j.1365-2486.2008.01736.x>

- Gruber, R. M. (2003). *Control and forecasting of the fructification of European beech (Fagus sylvatica L.) for the stand Zierenberg 38A and the level I stand in Hessen by climate factors.* <https://publications.goettingen-research-online.de/handle/2/46087>
- Hackett-Pain, A., Foest, J. J., Pearse, I. S., LaMontagne, J. M., Koenig, W. D., Vacchiano, G., Bogdziewicz, M., Caignard, T., Celebias, P., van Dormolen, J., Fernández-Martínez, M., Moris, J. V., Palaghianu, C., Pesendorfer, M., Satake, A., Schermer, E., Tanentzap, A. J., Thomas, P. A., Vecchio, D., ... Ascoli, D. (2022). MASTREE+: Time-series of plant reproductive effort from six continents. *Global Change Biology*, 28(9), 3066–3082. <https://doi.org/10.1111/gcb.16130>
- Hartig, F., & Lohse, L. (2022). *DHARMA: Residual Diagnostics for Hierarchical (Multi-Level / Mixed) Regression Models* (0.4.6) [Computer software]. <https://cran.r-project.org/web/packages/DHARMA/index.html>
- Hasselquist, N. J., Metcalfe, D. B., Inselsbacher, E., Stangl, Z., Oren, R., Näsholm, T., & Högberg, P. (2016). Greater carbon allocation to mycorrhizal fungi reduces tree nitrogen uptake in a boreal forest. *Ecology*, 97(4), 1012–1022. <https://doi.org/10.1890/15-1222.1>
- Hiltbrunner, E., Körner, C., Meier, R., Braun, S., & Kahmen, A. (2019). Data do not support large-scale oligotrophication of terrestrial ecosystems. *Nature Ecology & Evolution*, 3(9), Article 9. <https://doi.org/10.1038/s41559-019-0948-5>
- Hobbie, E. A., Bendiksen, K., Thorp, N. R., Ohenoja, E., & Ouimette, A. P. (2021). Climate Records, Isotopes, and C:N Stoichiometry Reveal Carbon and Nitrogen Flux Dynamics Differ Between Functional Groups of Ectomycorrhizal Fungi. *Ecosystems*. <https://doi.org/10.1007/s10021-021-00710-z>
- Hobbie, E. A., Chen, J., & Hasselquist, N. J. (2019). Fertilization alters nitrogen isotopes and concentrations in ectomycorrhizal fungi and soil in pine forests. *Fungal Ecology*, 39, 267–275. <https://doi.org/10.1016/j.funeco.2018.12.013>
- Hobbie, E. A., & Colpaert, J. V. (2003). Nitrogen availability and colonization by mycorrhizal fungi correlate with nitrogen isotope patterns in plants. *New Phytologist*, 157(1), 115–126. <https://doi.org/10.1046/j.1469-8137.2003.00657.x>
- Hobbie, E. A., Grandy, A. S., & Harmon, M. E. (2020). Isotopic and compositional evidence for carbon and nitrogen dynamics during wood decomposition by saprotrophic fungi. *Fungal Ecology*, 45, 100915. <https://doi.org/10.1016/j.funeco.2020.100915>
- Hobbie, E. A., & Högberg, P. (2012). Nitrogen isotopes link mycorrhizal fungi and plants to nitrogen dynamics. *New Phytologist*, 196(2), 367–382. <https://doi.org/10.1111/j.1469-8137.2012.04300.x>
- Hobbie, E. A., Ouimette, A. P., Schuur, E. A. G., Kierstead, D., Trappe, J. M., Bendiksen, K., & Ohenoja, E. (2013). Radiocarbon evidence for the mining of organic nitrogen from soil by mycorrhizal fungi. *Biogeochemistry*, 114(1), 381–389. <https://doi.org/10.1007/s10533-012-9779-z>
- Hobbie, E. A., Rice, S. F., Weber, N. S., & Smith, J. E. (2016). Isotopic evidence indicates saprotrophy in post-fire Morchella in Oregon and Alaska. *Mycologia*, 108(4), 638–645. <https://doi.org/10.3852/15-281>

- Hobbie, E. A., Weber, N. S., Trappe, J. M., & Van Klinken, G. J. (2002). Using radiocarbon to determine the mycorrhizal status of fungi. *New Phytologist*, *156*(1), 129–136. <https://doi.org/10.1046/j.1469-8137.2002.00496.x>
- Hoeksema, J. D., Chaudhary, V. B., Gehring, C. A., Johnson, N. C., Karst, J., Koide, R. T., Pringle, A., Zabinski, C., Bever, J. D., Moore, J. C., Wilson, G. W. T., Klironomos, J. N., & Umbanhowar, J. (2010). A meta-analysis of context-dependency in plant response to inoculation with mycorrhizal fungi. *Ecology Letters*, *13*(3), 394–407. <https://doi.org/10.1111/j.1461-0248.2009.01430.x>
- Högberg, M. N., Briones, M. J. I., Keel, S. G., Metcalfe, D. B., Campbell, C., Midwood, A. J., Thornton, B., Hurry, V., Linder, S., Näsholm, T., & Högberg, P. (2010). Quantification of effects of season and nitrogen supply on tree below-ground carbon transfer to ectomycorrhizal fungi and other soil organisms in a boreal pine forest. *New Phytologist*, *187*(2), 485–493. <https://doi.org/10.1111/j.1469-8137.2010.03274.x>
- Högberg, P., Johannisson, C., Yarwood, S., Callesen, I., Näsholm, T., Myrold, D. D., & Högberg, M. N. (2011). Recovery of ectomycorrhiza after ‘nitrogen saturation’ of a conifer forest. *New Phytologist*, *189*(2), 515–525. <https://doi.org/10.1111/j.1469-8137.2010.03485.x>
- Högberg, P., Näsholm, T., Franklin, O., & Högberg, M. N. (2017). Tamm Review: On the nature of the nitrogen limitation to plant growth in Fennoscandian boreal forests. *Forest Ecology and Management*, *403*, 161–185. <https://doi.org/10.1016/j.foreco.2017.04.045>
- Högberg, P., Nordgren, A., Buchmann, N., Taylor, A. F. S., Ekblad, A., Högberg, M. N., Nyberg, G., Ottosson-Löfvenius, M., & Read, D. J. (2001). Large-scale forest girdling shows that current photosynthesis drives soil respiration. *Nature*, *411*(6839), Article 6839. <https://doi.org/10.1038/35081058>
- Huo, C., Luo, Y., & Cheng, W. (2017). Rhizosphere priming effect: A meta-analysis. *Soil Biology and Biochemistry*, *111*, 78–84. <https://doi.org/10.1016/j.soilbio.2017.04.003>
- Jonard, M., Fürst, A., Verstraeten, A., Thimonier, A., Timmermann, V., Potočić, N., Waldner, P., Benham, S., Hansen, K., Merilä, P., Ponette, Q., Cruz, A. C. de la, Roskams, P., Nicolas, M., Croisé, L., Ingerslev, M., Matteucci, G., Decinti, B., Bascietto, M., & Rautio, P. (2015). Tree mineral nutrition is deteriorating in Europe. *Global Change Biology*, *21*(1), 418–430. <https://doi.org/10.1111/gcb.12657>
- Jørgensen, K., Clemmensen, K. E., Wallander, H., & Lindahl, B. D. (2023). Do ectomycorrhizal exploration types reflect mycelial foraging strategies? *New Phytologist*, *237*(2), 576–584. <https://doi.org/10.1111/nph.18566>
- Karst, J., Wasylwi, J., Birch, J. D., Franklin, J., Chang, S. X., & Erbilgin, N. (2021). Long-term nitrogen addition does not sustain host tree stem radial growth but doubles the abundance of high-biomass ectomycorrhizal fungi. *Global Change Biology*, *27*(17), 4125–4138. <https://doi.org/10.1111/gcb.15713>
- Keeling, C. D. (1979). The Suess effect: ¹³Carbon-¹⁴Carbon interrelations. *Environment International*, *2*(4), 229–300. [https://doi.org/10.1016/0160-4120\(79\)90005-9](https://doi.org/10.1016/0160-4120(79)90005-9)

- Kelly, D. (1994). The evolutionary ecology of mast seeding. *Trends in Ecology & Evolution*, 9(12), 465–470. [https://doi.org/10.1016/0169-5347\(94\)90310-7](https://doi.org/10.1016/0169-5347(94)90310-7)
- Knowles, J. E., & Frederick, C. (2016). merTools: Tools for analyzing mixed effect regression models. *R Package Version 0.3. 0*.
- Knudson, H., & Versterholt, J. (2008). *Funga Nordica: Agaricoid, boletoid and cyphelloid genera*. Nordsvamp.
- Koenig, W. D., & Knops, J. M. H. (1998). Scale of mast-seeding and tree-ring growth. *Nature*, 396(6708), Article 6708. <https://doi.org/10.1038/24293>
- Koide, R. T., Fernandez, C., & Malcolm, G. (2014). Determining place and process: Functional traits of ectomycorrhizal fungi that affect both community structure and ecosystem function. *New Phytologist*, 201(2), 433–439. <https://doi.org/10.1111/nph.12538>
- Kranabetter, J. M., Harman-Denhoed, R., & Hawkins, B. J. (2019). Saprotrophic and ectomycorrhizal fungal sporocarp stoichiometry (C: N: P) across temperate rainforests as evidence of shared nutrient constraints among symbionts. *New Phytologist*, 221(1), 482–492. <https://doi.org/10.1111/nph.15380>
- Kuo, M., & Methven, A. (2014). *Mushrooms of the Midwest*. Univ of Illinois Press.
- Kuznetsova, A., Brockhoff, P. B., & Christensen, R. H. B. (2017). lmerTest Package: Tests in Linear Mixed Effects Models. *Journal of Statistical Software*, 82, 1–26. <https://doi.org/10.18637/jss.v082.i13>
- Leavitt, S. W., & Lara, A. (1994). *South American tree rings show declining $\delta^{13}C$ trend* (2). 46(2), Article 2. <https://doi.org/10.3402/tellusb.v46i2.15760>
- Lilleskov, E. A., Hobbie, E. A., & Fahey, T. J. (2002). Ectomycorrhizal fungal taxa differing in response to nitrogen deposition also differ in pure culture organic nitrogen use and natural abundance of nitrogen isotopes. *New Phytologist*, 154(1), 219–231. <https://doi.org/10.1046/j.1469-8137.2002.00367.x>
- Lilleskov, E. A., Hobbie, E. A., & Horton, T. R. (2011). Conservation of ectomycorrhizal fungi: Exploring the linkages between functional and taxonomic responses to anthropogenic N deposition. *Fungal Ecology*, 4(2), 174–183. <https://doi.org/10.1016/j.funeco.2010.09.008>
- Lilleskov, E. A., Kuyper, T. W., Bidartondo, M. I., & Hobbie, E. A. (2019). Atmospheric nitrogen deposition impacts on the structure and function of forest mycorrhizal communities: A review. *Environmental Pollution*, 246, 148–162. <https://doi.org/10.1016/j.envpol.2018.11.074>
- Lindahl, B. D., & Tunlid, A. (2015). Ectomycorrhizal fungi – potential organic matter decomposers, yet not saprotrophs. *New Phytologist*, 205(4), 1443–1447. <https://doi.org/10.1111/nph.13201>
- Long, J. A. (2023). *jtools: Analysis and Presentation of Social Scientific Data* (2.2.2) [Computer software]. <https://cran.r-project.org/web/packages/jtools/index.html>
- Lüdtke, D. (2018). ggeffects: Tidy Data Frames of Marginal Effects from Regression Models. *Journal of Open Source Software*, 3(26), 772. <https://doi.org/10.21105/joss.00772>
- Mason, R. E., Craine, J. M., Lany, N. K., Jonard, M., Ollinger, S. V., Groffman, P. M., Fulweiler, R. W., Angerer, J., Read, Q. D., Reich, P. B., Templer, P. H., & Elmore,

- A. J. (2022). Evidence, causes, and consequences of declining nitrogen availability in terrestrial ecosystems. *Science*, 376(6590), eabh3767. <https://doi.org/10.1126/science.abh3767>
- McLauchlan, K. K., Ferguson, C. J., Wilson, I. E., Ocheltree, T. W., & Craine, J. M. (2010). Thirteen decades of foliar isotopes indicate declining nitrogen availability in central North American grasslands. *New Phytologist*, 187(4), 1135–1145. <https://doi.org/10.1111/j.1469-8137.2010.03322.x>
- Mohan, J. E., Cowden, C. C., Baas, P., Dawadi, A., Frankson, P. T., Helmick, K., Hughes, E., Khan, S., Lang, A., Machmuller, M., Taylor, M., & Witt, C. A. (2014). Mycorrhizal fungi mediation of terrestrial ecosystem responses to global change: Mini-review. *Fungal Ecology*, 10, 3–19. <https://doi.org/10.1016/j.funeco.2014.01.005>
- Muggeo, V. (2008). Segmented: An R package to fit regression models with broken-line relationships. *R News*, 8(1), 20–25.
- Muhr, J., Messier, C., Delagrangé, S., Trumbore, S., Xu, X., & Hartmann, H. (2016). How fresh is maple syrup? Sugar maple trees mobilize carbon stored several years previously during early springtime sap-ascent. *New Phytologist*, 209(4), 1410–1416. <https://doi.org/10.1111/nph.13782>
- Nakahata, R., Naramoto, M., Sato, M., & Mizunaga, H. (2021). Multifunctions of fine root phenology in vegetative and reproductive growth in mature beech forest ecosystems. *Ecosphere*, 12(10), e03788. <https://doi.org/10.1002/ecs2.3788>
- Näsholm, T., Höglberg, P., Franklin, O., Metcalfe, D., Keel, S. G., Campbell, C., Hurry, V., Linder, S., & Höglberg, M. N. (2013). Are ectomycorrhizal fungi alleviating or aggravating nitrogen limitation of tree growth in boreal forests? *The New Phytologist*, 198(1), 214–221. <https://doi.org/10.1111/nph.12139>
- Newsham, K. K., Garnett, M. H., Robinson, C. H., & Cox, F. (2018). Discrete taxa of saprotrophic fungi respire different ages of carbon from Antarctic soils. *Scientific Reports*, 8(1), Article 1. <https://doi.org/10.1038/s41598-018-25877-9>
- Nikolova, P. S., Zang, C., & Pretzsch, H. (2011). Combining tree-ring analyses on stems and coarse roots to study the growth dynamics of forest trees: A case study on Norway spruce (*Picea abies* [L.] H. Karst). *Trees*, 25(5), 859–872. <https://doi.org/10.1007/s00468-011-0561-y>
- Nussbaumer, A., Waldner, P., Etzold, S., Gessler, A., Benham, S., Thomsen, I. M., Jørgensen, B. B., Timmermann, V., Verstraeten, A., Sioen, G., Rautio, P., Ukonmaanaho, L., Skudnik, M., Apuhtin, V., Braun, S., & Wauer, A. (2016). Patterns of mast fruiting of common beech, sessile and common oak, Norway spruce and Scots pine in Central and Northern Europe. *Forest Ecology and Management*, 363, 237–251. <https://doi.org/10.1016/j.foreco.2015.12.033>
- Ostfeld, R. S., Keesing, F., Ostfeld, R. S., & Keesing, F. (2000). Pulsed resources and community dynamics of consumers in terrestrial ecosystems. *Trends in Ecology & Evolution*, 15(6), 232–237. [https://doi.org/10.1016/S0169-5347\(00\)01862-0](https://doi.org/10.1016/S0169-5347(00)01862-0)
- Paradis, E., & Schliep, K. (2019). ape 5.0: An environment for modern phylogenetics and evolutionary analyses in R. *Bioinformatics*, 35(3), 526–528. <https://doi.org/10.1093/bioinformatics/bty633>

- Pearse, I. S., Koenig, W. D., & Kelly, D. (2016). Mechanisms of mast seeding: Resources, weather, cues, and selection. *New Phytologist*, *212*(3), 546–562. <https://doi.org/10.1111/nph.14114>
- Pearse, I. S., LaMontagne, J. M., Lordon, M., Hipp, A. L., & Koenig, W. D. (2020). Biogeography and phylogeny of masting: Do global patterns fit functional hypotheses? *New Phytologist*, *227*(5), 1557–1567. <https://doi.org/10.1111/nph.16617>
- Pellitier, P. T., Ibáñez, I., Zak, D. R., Argiroff, W. A., & Acharya, K. (2021). Ectomycorrhizal access to organic nitrogen mediates CO₂ fertilization response in a dominant temperate tree. *Nature Communications*, *12*(1), 5403. <https://doi.org/10.1038/s41467-021-25652-x>
- Pesendorfer, M. B., Ascoli, D., Bogdziewicz, M., Hacket-Pain, A., Pearse, I. S., & Vacchiano, G. (2021). The ecology and evolution of synchronized reproduction in long-lived plants. *Philosophical Transactions of the Royal Society B: Biological Sciences*, *376*(1839), 20200369. <https://doi.org/10.1098/rstb.2020.0369>
- Phillips, R. P., Brzostek, E., & Midgley, M. G. (2013). The mycorrhizal-associated nutrient economy: A new framework for predicting carbon-nutrient couplings in temperate forests. *New Phytologist*, *199*(1), 41–51. <https://doi.org/10.1111/nph.12221>
- Pölme, S., Abarenkov, K., Henrik Nilsson, R., Lindahl, B. D., Clemmensen, K. E., Kauserud, H., Nguyen, N., Kjølner, R., Bates, S. T., Baldrian, P., Frøslev, T. G., Adojaan, K., Vizzini, A., Suija, A., Pfister, D., Baral, H.-O., Järv, H., Madrid, H., Nordén, J., ... Tedersoo, L. (2020). FungalTraits: A user-friendly traits database of fungi and fungus-like stramenopiles. *Fungal Diversity*, *105*(1), 1–16. <https://doi.org/10.1007/s13225-020-00466-2>
- Ponce, Á., Alday, J. G., Bonet, J. A., Martínez de Aragón, J., & de-Miguel, S. (2023). Fungal sporocarp productivity and diversity shaped by weather conditions in *Pinus uncinata* stands. *Forest Ecology and Management*, *545*, 121256. <https://doi.org/10.1016/j.foreco.2023.121256>
- R Core Team. (2023). *R: The R Project for Statistical Computing*. <https://www.r-project.org/>
- Robertson, I., Froyd, C. A., Walsh, R. P. D., Newbery, D. M., Woodborne, S., & Ong, R. C. (2004). The dating of dipterocarp tree rings: Establishing a record of carbon cycling and climatic change in the tropics. *Journal of Quaternary Science*, *19*(7), 657–664. <https://doi.org/10.1002/jqs.885>
- Sabadel, A., Durante, L., & Wing, S. (2020). Stable isotopes of amino acids from reef fishes uncover Suess and nitrogen enrichment effects on local ecosystems. *Marine Ecology Progress Series*, *647*, 149–160. <https://doi.org/10.3354/meps13414>
- Sato, H., Morimoto, S., & Hattori, T. (2012). A Thirty-Year Survey Reveals That Ecosystem Function of Fungi Predicts Phenology of Mushroom Fruiting. *PLoS ONE*, *7*(11), e49777. <https://doi.org/10.1371/journal.pone.0049777>
- Savard, M. M., Marion, J., Bégin, C., & Laganière, J. (2023). On the significance of long-term trends in tree-ring N isotopes – The interplay of soil conditions and regional NO_x emissions. *Science of The Total Environment*, *857*, 159580. <https://doi.org/10.1016/j.scitotenv.2022.159580>

- Schimel, J. P. (2018). Life in Dry Soils: Effects of Drought on Soil Microbial Communities and Processes. *Annual Review of Ecology, Evolution, and Systematics*, 49(1), 409–432. <https://doi.org/10.1146/annurev-ecolsys-110617-062614>
- Shah, F., Nicolás, C., Bentzer, J., Ellström, M., Smits, M., Rineau, F., Canbäck, B., Floudas, D., Carleer, R., Lackner, G., Braesel, J., Hoffmeister, D., Henrissat, B., Ahrén, D., Johansson, T., Hibbett, D. S., Martin, F., Persson, P., & Tunlid, A. (2016). Ectomycorrhizal fungi decompose soil organic matter using oxidative mechanisms adapted from saprotrophic ancestors. *New Phytologist*, 209(4), 1705–1719. <https://doi.org/10.1111/nph.13722>
- Smith, B. (2022). Declining global leaf nitrogen content: Smart resource use by flexible plants? *New Phytologist*, 235(5), 1683–1685. <https://doi.org/10.1111/nph.18354>
- Smith, S. E., & Read, D. J. (2010). *Mycorrhizal Symbiosis*. Academic Press.
- Soudzilovskaia, N. A., Vaessen, S., Barcelo, M., He, J., Rahimlou, S., Abarenkov, K., Brundrett, M. C., Gomes, S., Merckx, V., & Tedersoo, L. (2019). *FungalRoot: Global online database of plant mycorrhizal associations* (p. 717488). bioRxiv. <https://doi.org/10.1101/717488>
- Steidinger, B. S., Crowther, T. W., Liang, J., Van Nuland, M. E., Werner, G. D. A., Reich, P. B., Nabuurs, G. J., de-Miguel, S., Zhou, M., Picard, N., Herault, B., Zhao, X., Zhang, C., Routh, D., & Peay, K. G. (2019). Climatic controls of decomposition drive the global biogeography of forest-tree symbioses. *Nature*, 569(7756), 404–408. <https://doi.org/10.1038/s41586-019-1128-0>
- Stephens, R. B., Hobbie, E. A., Lee, T. D., & Rowe, R. J. (2019). Pulsed resource availability changes dietary niche breadth and partitioning between generalist rodent consumers. *Ecology and Evolution*, 9(18), 10681–10693. <https://doi.org/10.1002/ece3.5587>
- Straatsma, G., Ayer, F., & Egli, S. (2001). Species richness, abundance, and phenology of fungal fruit bodies over 21 years in a Swiss forest plot. *Mycological Research*, 105(5), 515–523. <https://doi.org/10.1017/S0953756201004154>
- Strien, A. J. van, Boomsluit, M., Noordeloos, M. E., Verweij, R. J. T., & Kuyper, T. W. (2018). Woodland ectomycorrhizal fungi benefit from large-scale reduction in nitrogen deposition in the Netherlands. *Journal of Applied Ecology*, 55(1), 290–298. <https://doi.org/10.1111/1365-2664.12944>
- Swart, P. K., Greer, L., Rosenheim, B. E., Moses, C. S., Waite, A. J., Winter, A., Dodge, R. E., & Helmle, K. (2010). The 13C Suess effect in scleractinian corals mirror changes in the anthropogenic CO2 inventory of the surface oceans. *Geophysical Research Letters*, 37(5). <https://doi.org/10.1029/2009GL041397>
- Tanentzap, A. J., Lee, W. G., & Coomes, D. A. (2012). Soil nutrient supply modulates temperature-induction cues in mast-seeding grasses. *Ecology*, 93(3), 462–469. <https://doi.org/10.1890/11-1750.1>
- Tedersoo, L., & Smith, M. E. (2013). Lineages of ectomycorrhizal fungi revisited: Foraging strategies and novel lineages revealed by sequences from belowground. *Fungal Biology Reviews*, 27(3), 83–99. <https://doi.org/10.1016/j.fbr.2013.09.001>

- Terrer, C., Vicca, S., Hungate, B. A., Phillips, R. P., & Prentice, I. C. (2016). Mycorrhizal association as a primary control of the CO₂ fertilization effect. *Science*, *353*(6294), 72–74. <https://doi.org/10.1126/science.aaf4610>
- Teste, F. P., Jones, M. D., & Dickie, I. A. (2020). Dual-mycorrhizal plants: Their ecology and relevance. *New Phytologist*, *225*(5), 1835–1851. <https://doi.org/10.1111/nph.16190>
- Unestam, T., & Sun, Y.-P. (1995). Extramatrical structures of hydrophobic and hydrophilic ectomycorrhizal fungi. *Mycorrhiza*, *5*(5), 301–311. <https://doi.org/10.1007/BF00207402>
- Vaario, L.-M., Sah, S. P., Norisada, M., Narimatsu, M., & Matsushita, N. (2019). *Tricholoma matsutake* may take more nitrogen in the organic form than other ectomycorrhizal fungi for its sporocarp development: The isotopic evidence. *Mycorrhiza*, *29*(1), 51–59. <https://doi.org/10.1007/s00572-018-0870-8>
- Vacchiano, G., Hacket-Pain, A., Turco, M., Motta, R., Maringer, J., Conedera, M., Drobyshev, I., & Ascoli, D. (2017). Spatial patterns and broad-scale weather cues of beech mast seeding in Europe. *New Phytologist*, *215*(2), 595–608. <https://doi.org/10.1111/nph.14600>
- van der Linde, S., Suz, L. M., Orme, C. D. L., Cox, F., Andreae, H., Asi, E., Atkinson, B., Benham, S., Carroll, C., Cools, N., De Vos, B., Dietrich, H.-P., Eichhorn, J., Gehrman, J., Grebenc, T., Gweon, H. S., Hansen, K., Jacob, F., Kristöfel, F., ... Bidartondo, M. I. (2018). Environment and host as large-scale controls of ectomycorrhizal fungi. *Nature*, *558*(7709), Article 7709. <https://doi.org/10.1038/s41586-018-0189-9>
- Wallander, H. (1995). A new hypothesis to explain allocation of dry matter between mycorrhizal fungi and pine seedlings in relation to nutrient supply. In L. O. Nilsson, R. F. Hüttel, & U. T. Johansson (Eds.), *Nutrient Uptake and Cycling in Forest Ecosystems: Proceedings of the CEC/IUFRO Symposium Nutrient Uptake and Cycling in Forest Ecosystems Halmstad, Sweden, June, 7–10, 1993* (pp. 243–248). Springer Netherlands. https://doi.org/10.1007/978-94-011-0455-5_27
- Zackrisson, O., Nilsson, M.-C., Jäderlund, A., & Wardle, D. A. (1999). Nutritional Effects of Seed Fall during Mast Years in Boreal Forest. *Oikos*, *84*(1), 17–26. <https://doi.org/10.2307/3546862>

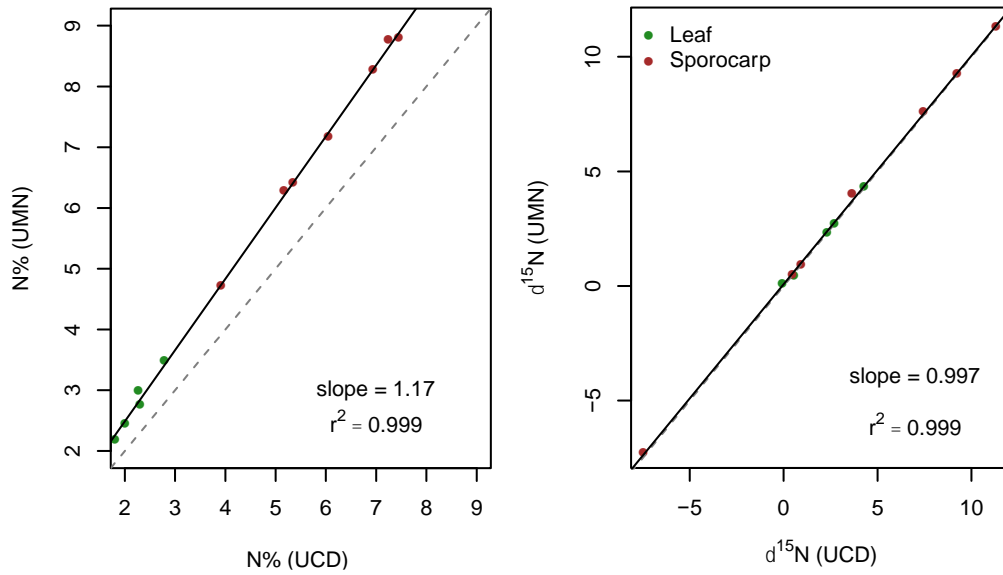
Appendices

Appendix S1.1. Herbarium specimen selection criteria, analysis protocols, and data quality control

Specimens were selected from a range of plant and fungal species. All specimens were sampled from collections present at the Bell Herbarium at the University of Minnesota. We identified plant and fungal genera that were collected across eight decades between 1880 and 2010 from a 130 km² surrounding the University of Minnesota St. Paul Campus. Samples were air dried, ground to a fine powder, and weighed for analysis. Isotopic standards included peach leaves, acetanilide elemental standard, and the USGS40 glutamic acid isotopic standard for $\delta^{15}\text{N}$.

Isotopic analyses of samples for this dataset were measured at one of two facilities: The University of Minnesota facility in the Gutknecht laboratory using an Elementar Vario Pyrocube (Hanau, Germany) interfaced to an Isoprime 100 isotope ratio mass spectrometer (Cheadle, UK), or at the University of California-Davis (UC-Davis) Stable Isotope facility, using an Elementar Vario EL Cube interfaced to a PDZ Europa 20-20 isotope ratio mass spectrometer (Sercon Ltd., Cheshire, UK). To eliminate concern over consistency of data between these two facilities, twelve herbarium specimens were analyzed at both facilities (Appendix S1.2). To correct for the difference in slopes in N concentrations (Appendix S1.2), N concentration values generated from the University of Minnesota facility in the Gutknecht laboratory were divided by the slope coefficient (1.17, Appendix S1.2). These corrected values were used in further analyses.

Appendix S1.2. Twelve herbarium specimens were analyzed at both UC-Davis and University of Minnesota isotope facilities, and comparisons of $\delta^{15}\text{N}$ and N concentrations are visualized. Gray dashed line represents the 1:1 line. Black line represents regression model, along with model slope and r^2 value.



Appendix S1.3. Summary of species-level herbarium collections from the Minnesota, USA, stored in the Bell Museum of Natural History, with reference to species, ecological group (EMF = ectomycorrhizal fungus, EMP = ectomycorrhizal plant, Sap = saprotrophic fungus, AMP = arbuscular mycorrhizal plant), and number of collections (n).

group	Genus	Species	n
EMF	<i>Laccaria</i>	<i>Laccaria_bicolor</i>	3
EMF	<i>Scleroderma</i>	<i>Scleroderma_citrinum</i>	3
Sap	<i>Lycoperdon</i>	<i>Lycoperdon_curtisii</i>	3
Sap	<i>Lycoperdon</i>	<i>Lycoperdon_gemmatum</i>	3
Sap	<i>Marasmius</i>	<i>Marasmius_delectans</i>	3
Sap	<i>Psathyrella</i>	<i>Psathyrella_echiniceps</i>	3
EMF	<i>Amanita</i>	<i>Amanita_rubescens</i>	4
EMF	<i>Scleroderma</i>	<i>Scleroderma_bovista</i>	4
Sap	<i>Marasmius</i>	<i>Marasmius_androsaceus</i>	4
EMF	<i>Amanita</i>	<i>Amanita_phalloides</i>	5
Sap	<i>Marasmius</i>	<i>Marasmius_oreades</i>	5
EMF	<i>Amanita</i>	<i>Amanita_pantherina</i>	6
EMF	<i>Scleroderma</i>	<i>Scleroderma_areolatum</i>	6
Sap	<i>Marasmius</i>	<i>Marasmius_rotula</i>	6
Sap	<i>Marasmius</i>	<i>Marasmius_scorodoni</i>	6
EMF	<i>Laccaria</i>	<i>Laccaria_ochropurpurea</i>	7
Sap	<i>Marasmius</i>	<i>Marasmius_siccus</i>	7
EMF	<i>Scleroderma</i>	<i>Scleroderma_cepa</i>	8
EMP	<i>Betula</i>	<i>Betula_alleghaniensis</i>	8
EMF	<i>Laccaria</i>	<i>Laccaria_amethystina</i>	9
AMP	<i>Juglans</i>	<i>Juglans_nigra</i>	11
EMF	<i>Amanita</i>	<i>Amanita_vaginata</i>	11
AMP	<i>Ulmus</i>	<i>Ulmus_americanus</i>	13
Sap	<i>Psathyrella</i>	<i>Psathyrella_candolleana</i>	13
AMP	<i>Ulmus</i>	<i>Ulmus_rubra</i>	14
EMF	<i>Laccaria</i>	<i>Laccaria_laccata</i>	14
AMP	<i>Acer</i>	<i>Acer_negundo</i>	15
AMP	<i>Acer</i>	<i>Acer_saccharinum</i>	15
EMF	<i>Amanita</i>	<i>Amanita_bisporigera</i>	18
EMP	<i>Populus</i>	<i>Populus_tremuloides</i>	18
Sap	<i>Lycoperdon</i>	<i>Lycoperdon_pyrriforme</i>	18
EMP	<i>Betula</i>	<i>Betula_papyrifera</i>	19
EMP	<i>Populus</i>	<i>Populus_grandidentata</i>	19
AMP	<i>Juglans</i>	<i>Juglans_cinerea</i>	20

AMP	<i>Acer</i>	<i>Acer_saccharum</i>	21
EMP	<i>Betula</i>	<i>Betula_pumila</i>	24
AMP	<i>Prunus</i>	<i>Prunus_virginiana</i>	28
EMP	<i>Ostrya</i>	<i>Ostrya_virginiana</i>	29
EMP	<i>Tilia</i>	<i>Tilia_americana</i>	34
AMP	<i>Fraxinus</i>	<i>Fraxinus_pennsylvanica</i>	36

Appendix S1.4. Summary of species-level foliar data analyzed from across the United States, with reference to genus, species, number of samples (n), and mycorrhizal type (Mycorrhizal).

Genus	Species	Mycorrhizal	n
<i>Abies</i>	<i>Abies balsamea</i>	Ecto	10
<i>Abies</i>	<i>Abies balsamifera</i>	Ecto	2
<i>Abies</i>	<i>Abies concolor</i>	Ecto	2
<i>Abies</i>	<i>Abies grandis</i>	Ecto	2
<i>Abies</i>	<i>Abies lasiocarpa</i>	Ecto	2
<i>Acer</i>	<i>Acer circinatum</i>	AM	7
<i>Acer</i>	<i>Acer grandidentatum</i>	AM	11
<i>Acer</i>	<i>Acer negundo</i>	AM	12
<i>Acer</i>	<i>Acer pensylvanicum</i>	AM	3
<i>Acer</i>	<i>Acer rubrum</i>	AM	12
<i>Acer</i>	<i>Acer saccharinum</i>	AM	1
<i>Acer</i>	<i>Acer saccharum</i>	AM	18
<i>Acer</i>	<i>Acer spp.</i>	AM	1
<i>Achillea</i>	<i>Achillea lanulosa</i>	AM	1
<i>Achillea</i>	<i>Achillea millefolium</i>	AM	1
<i>Achlys</i>	<i>Achlys triphylla</i>	AM	4
<i>Achnatherum</i>	<i>Achnatherum hymenoides</i>	AM	1
<i>Acomastylis</i>	<i>Acomastylis</i>	AM	2
<i>Adenocaulon</i>	<i>Adenocaulon bicolor</i>	AM	6
<i>Adenostoma</i>	<i>Adenostoma fasciculatum</i>	AM	1
<i>Aesculus</i>	<i>Aesculus californica</i>	AM	1
<i>Agoseris</i>	<i>Agoseris glauca</i>	AM	1
<i>Agropyron</i>	<i>Agropyron desertorum</i>	AM	1
<i>Ambrosia</i>	<i>Ambrosia artemisiifolia</i>	AM	2
<i>Ambrosia</i>	<i>Ambrosia dumosa</i>	AM	2
<i>Ambrosia</i>	<i>Ambrosia psilostachya</i>	AM	3
<i>Ambrosia</i>	<i>Ambrosia tomentosa</i>	AM	1
<i>Anaphalis</i>	<i>Anaphalis margaritacea</i>	AM	7
<i>Androsace</i>	<i>Androsace septentrionalis</i>	AM	1
<i>Antennaria</i>	<i>Antennaria parvifolia</i>	AM	1
<i>Antennaria</i>	<i>Antennaria rosulata</i>	AM	2
<i>Aristida</i>	<i>Aristida purpurea</i>	AM	1
<i>Artemisia</i>	<i>Artemisia</i>	AM	2
<i>Artemisia</i>	<i>Artemisia dracuncululus</i>	AM	7
<i>Artemisia</i>	<i>Artemisia dracuncululus</i>	AM	8
<i>Artemisia</i>	<i>Artemisia ludoviciana</i>	AM	8

<i>Artemisia</i>	<i>Artemisia californica</i>	AM	1
<i>Artemisia</i>	<i>Artemisia campestris</i>	AM	1
<i>Artemisia</i>	<i>Artemisia cana</i>	AM	2
<i>Artemisia</i>	<i>Artemisia carruthii</i>	AM	1
<i>Artemisia</i>	<i>Artemisia dracunculus</i>	AM	1
<i>Artemisia</i>	<i>Artemisia frigida</i>	AM	7
<i>Artemisia</i>	<i>Artemisia tridentata</i>	AM	1
<i>Artemisia</i>	<i>Artemisia tridentata var. vaseyana</i>	AM	1
<i>Asarum</i>	<i>Asarum caudatum</i>	AM	6
<i>Asyneuma</i>	<i>Asyneuma prenanthoides</i>	AM	5
<i>Baccharis</i>	<i>Baccharis pilularis</i>	AM	1
<i>Bahia</i>	<i>Bahia dissecta</i>	AM	1
<i>Betula</i>	<i>Betula alleghaniensis</i>	Ecto	17
<i>Betula</i>	<i>Betula allegheniensis</i>	Ecto	1
<i>Betula</i>	<i>Betula occidentalis</i>	Ecto	19
<i>Betula</i>	<i>Betula papyrifera</i>	Ecto	13
<i>Betula</i>	<i>Betula populifolia</i>	Ecto	1
<i>Bistorta</i>	<i>Bistorta</i>	Ecto	2
<i>Blechnum</i>	<i>Blechnum spicant</i>	AM	3
<i>Blepharoneuron</i>	<i>Blepharoneuron tricholepis</i>	AM	1
<i>Bouteloua</i>	<i>Bouteloua curtipendula</i>	AM	1
<i>Bromus</i>	<i>Bromus anomalus</i>	AM	1
<i>Bromus</i>	<i>Bromus ciliatus</i>	AM	1
<i>Bromus</i>	<i>Bromus diandrus</i>	AM	1
<i>Bromus</i>	<i>Bromus tectorum</i>	AM	1
<i>Bromus</i>	<i>Bromus vulgaris</i>	AM	6
<i>Calamagrostis</i>	<i>Calamagrostis</i>	AM	1
<i>Calocedrus</i>	<i>Calocedrus decurrens</i>	AM	2
<i>Campanula</i>	<i>Campanula scouleri</i>	AM	7
<i>Carduus</i>	<i>Carduus pycnocephalus</i>	AM	1
<i>Carex</i>	<i>Carex</i>	AM	2
<i>Carex</i>	<i>Carex deweyana</i>	AM	4
<i>Carex</i>	<i>Carex geophila</i>	AM	1
<i>Carex</i>	<i>Carex geyeri</i>	AM	9
<i>Carex</i>	<i>Carex hendersonii</i>	AM	5
<i>Castilleja</i>	<i>Castilleja austromontana</i>	Ecto	1
<i>Castilleja</i>	<i>Castilleja integra</i>	Ecto	1
<i>Centaurea</i>	<i>Centaurea diffusa</i>	AM	1
<i>Centaurea</i>	<i>Centaurea solstitialis</i>	AM	1

<i>Chaetopappa</i>	<i>Chaetopappa ericoides</i>	AM	1
<i>Chamerion</i>	<i>Chamerion angustifolium</i>	AM	4
<i>Cheirodendron</i>	<i>Cheirodendron trigynum</i>	AM	1
<i>Chondrosium</i>	<i>Chondrosium gracile</i>	AM	1
<i>Chondrosium</i>	<i>Chondrosium simplex</i>	AM	1
<i>Chrysopsis</i>	<i>Chrysopsis villosa</i>	AM	1
<i>Chrysothamnus</i>	<i>Chrysothamnus nauseosus</i>	AM	1
<i>Cirsium</i>	<i>Cirsium wheeleri</i>	AM	2
<i>Claytonia</i>	<i>Claytonia perfoliata</i>	AM	2
<i>Claytonia</i>	<i>Claytonia sibirica</i>	AM	7
<i>Collomia</i>	<i>Collomia heterophylla</i>	AM	4
<i>Convolvulus</i>	<i>Convolvulus arvensis</i>	AM	1
<i>Coreopsis</i>	<i>Coreopsis tinctoria</i>	AM	1
<i>Cornus</i>	<i>Cornus stolonifera</i>	AM	19
<i>Corylus</i>	<i>Corylus cornuta</i>	AM	4
<i>Cosmos</i>	<i>Cosmos parviflorus</i>	AM	1
<i>Cyperus</i>	<i>Cyperus fendlerianus</i>	AM	1
<i>Dieteria</i>	<i>Dieteria canescens</i>	AM	1
<i>Digitalis</i>	<i>Digitalis purpurea</i>	AM	5
<i>Disporum</i>	<i>Disporum spp.</i>	AM	7
<i>Distichlis</i>	<i>Distichlis spicata</i>	AM	2
<i>Echeandia</i>	<i>Echeandia flavescens</i>	AM	1
<i>Elymus</i>	<i>Elymus elymoides</i>	AM	2
<i>Elymus</i>	<i>Elymus glaucus</i>	AM	7
<i>Elymus</i>	<i>Elymus smithii</i>	AM	1
<i>Elymus</i>	<i>Elymus trachycaulus</i>	AM	1
<i>Epilobium</i>	<i>Epilobium brachycarpum</i>	AM	1
<i>Epilobium</i>	<i>Epilobium latifolia</i>	AM	1
<i>Eragrostis</i>	<i>Eragrostis mexicana</i>	AM	1
<i>Ericameria</i>	<i>Ericameria</i>	AM	2
<i>Erigeron</i>	<i>Erigeron divergens</i>	AM	1
<i>Erigeron</i>	<i>Erigeron flagellaris</i>	AM	1
<i>Erigeron</i>	<i>Erigeron formosissimus</i>	AM	1
<i>Erigeron</i>	<i>Erigeron speciosus</i>	AM	1
<i>Erodium</i>	<i>Erodium cicutarium</i>	AM	1
<i>Euphorbia</i>	<i>Euphorbia brachycera</i>	AM	1
<i>Euphorbia</i>	<i>Euphorbia fendleri</i>	AM	1
<i>Euphorbia</i>	<i>Euphorbia serpyllifolia</i>	AM	1
<i>Fagus</i>	<i>Fagus grandifolia</i>	Ecto	15

<i>Festuca</i>	<i>Festuca</i>	AM	2
<i>Festuca</i>	<i>Festuca arizonica</i>	AM	2
<i>Festuca</i>	<i>Festuca occidentalis</i>	AM	6
<i>Fragaria</i>	<i>Fragaria virginiana</i>	AM	1
<i>Fraxinus</i>	<i>Fraxinus americana</i>	AM	2
<i>Fraxinus</i>	<i>Fraxinus nigra</i>	AM	1
<i>Fraxinus</i>	<i>Fraxinus pennsylvanica</i>	AM	1
<i>Gaillardia</i>	<i>Gaillardia pinnatifida</i>	AM	1
<i>Galium</i>	<i>Galium triflorum</i>	AM	6
<i>Geranium</i>	<i>Geranium caespitosum</i>	AM	1
<i>Geranium</i>	<i>Geranium richardsonii</i>	AM	2
<i>Geum</i>	<i>Geum triflorum</i>	AM	1
<i>Gutierrezia</i>	<i>Gutierrezia sarothrae</i>	AM	1
<i>Helianthella</i>	<i>Helianthella quinquenervis</i>	AM	1
<i>Helianthus</i>	<i>Helianthus annuus</i>	AM	1
<i>Heliomeris</i>	<i>Heliomeris multiflora</i>	AM	1
<i>Heteromeles</i>	<i>Heteromeles arbutifolia</i>	AM	1
<i>Hieracium</i>	<i>Hieracium albiflorum</i>	AM	7
<i>Hieracium</i>	<i>Hieracium fendleri</i>	AM	1
<i>Holodiscus</i>	<i>Holodiscus discolor</i>	AM	6
<i>Houstonia</i>	<i>Houstonia wrightii</i>	AM	1
<i>Hymenopappus</i>	<i>Hymenopappus mexicanus</i>	AM	1
<i>Hymenoxys</i>	<i>Hymenoxys hoopesii</i>	AM	1
<i>Hymenoxys</i>	<i>Hymenoxys richardsonii</i>	AM	1
<i>Hypericum</i>	<i>Hypericum perforatum</i>	AM	6
<i>Hypochaeris</i>	<i>Hypochaeris radicata</i>	AM	7
<i>Ipomopsis</i>	<i>Ipomopsis aggregata</i>	AM	1
<i>Ipomopsis</i>	<i>Ipomopsis multiflora</i>	AM	1
<i>Iris</i>	<i>Iris missouriensis</i>	AM	1
<i>Iris</i>	<i>Iris tenax</i>	AM	7
<i>Juglans</i>	<i>Juglans californica</i>	AM	1
<i>Juniperus</i>	<i>Juniperus monosperma</i>	AM	3
<i>Juniperus</i>	<i>Juniperus virginiana</i>	AM	1
<i>Koeleria</i>	<i>Koeleria macrantha</i>	AM	1
<i>Laennecia</i>	<i>Laennecia schiedeana</i>	AM	1
<i>Larix</i>	<i>Larix laricina</i>	Ecto	1
<i>Larix</i>	<i>Larix lyalli</i>	Ecto	1
<i>Linaria</i>	<i>Linaria dalmatica</i>	AM	1
<i>Linnaea</i>	<i>Linnaea borealis</i>	AM	3

<i>Linum</i>	<i>Linum australe</i>	AM	1
<i>Linum</i>	<i>Linum lewisii</i>	AM	1
<i>Lithospermum</i>	<i>Lithospermum multiflorum</i>	AM	1
<i>Luetkea</i>	<i>Luetkea pectinata</i>	AM	1
<i>Lycium</i>	<i>Lycium andersonii</i>	AM	1
<i>Lycium</i>	<i>Lycium pallida</i>	AM	1
<i>Mahonia</i>	<i>Mahonia nervosa</i>	AM	7
<i>Mertensia</i>	<i>Mertensia</i>	AM	2
<i>Muhlenbergia</i>	<i>Muhlenbergia minutissima</i>	AM	1
<i>Muhlenbergia</i>	<i>Muhlenbergia montana</i>	AM	1
<i>Muhlenbergia</i>	<i>Muhlenbergia ramulosa</i>	AM	1
<i>Muhlenbergia</i>	<i>Muhlenbergia rigens</i>	AM	1
<i>Muhlenbergia</i>	<i>Muhlenbergia wrightii</i>	AM	1
<i>Munroa</i>	<i>Munroa squarrosa</i>	AM	1
<i>Mycelis</i>	<i>Mycelis muralis</i>	AM	7
<i>Nama</i>	<i>Nama dichotomum</i>	AM	1
<i>Notholithocarpus</i>	<i>Notholithocarpus densiflorus</i>	Ecto	1
<i>Oenothera</i>	<i>Oenothera pubescens</i>	AM	1
<i>Osmorhiza</i>	<i>Osmorhiza berteroi</i>	AM	6
<i>Otleya</i>	<i>Otleya wrightii</i>	AM	1
<i>Oxalis</i>	<i>Oxalis alpina</i>	AM	1
<i>Oxalis</i>	<i>Oxalis oregana</i>	AM	7
<i>Packera</i>	<i>Packera multilobata</i>	AM	1
<i>Penstemon</i>	<i>Penstemon barbatus</i>	AM	1
<i>Penstemon</i>	<i>Penstemon linarioides</i>	AM	1
<i>Penstemon</i>	<i>Penstemon virgatus</i>	AM	1
<i>Phalaris</i>	<i>Phalaris arundinacea</i>	AM	6
<i>Phlox</i>	<i>Phlox speciosa</i>	AM	1
<i>Physocarpus</i>	<i>Physocarpus opulifolius</i>	AM	6
<i>Picea</i>	<i>Picea engelmannii</i>	Ecto	9
<i>Picea</i>	<i>Picea rubens</i>	Ecto	22
<i>Pinus</i>	<i>Pinus banksiana</i>	Ecto	11
<i>Pinus</i>	<i>Pinus contorta</i>	Ecto	1
<i>Pinus</i>	<i>Pinus edulis</i>	Ecto	3
<i>Pinus</i>	<i>Pinus eliottii</i>	Ecto	2
<i>Pinus</i>	<i>Pinus lambertiana</i>	Ecto	2
<i>Pinus</i>	<i>Pinus mariana</i>	Ecto	2
<i>Pinus</i>	<i>Pinus monophylla</i>	Ecto	1
<i>Pinus</i>	<i>Pinus palustris</i>	Ecto	1

<i>Pinus</i>	<i>Pinus ponderosa</i>	Ecto	4
<i>Pinus</i>	<i>Pinus resinosa</i>	Ecto	6
<i>Pinus</i>	<i>Pinus rigida</i>	Ecto	1
<i>Pinus</i>	<i>Pinus stroba</i>	Ecto	2
<i>Pinus</i>	<i>Pinus strobus</i>	Ecto	2
<i>Pinus</i>	<i>Pinus taeda</i>	Ecto	3
<i>Plantago</i>	<i>Plantago argyrea</i>	AM	1
<i>Plantago</i>	<i>Plantago lanceolata</i>	AM	1
<i>Pleuraphis</i>	<i>Pleuraphis rigida</i>	AM	1
<i>Poa</i>	<i>Poa compressa</i>	AM	1
<i>Poa</i>	<i>Poa fendleriana</i>	AM	1
<i>Poa</i>	<i>Poa pratensis</i>	AM	2
<i>Polygonum</i>	<i>Polygonum aviculare</i>	AM	1
<i>Polygonum</i>	<i>Polygonum douglasii</i>	AM	1
<i>Polypodium</i>	<i>Polypodium glycyrrhiza</i>	AM	2
<i>Polystichum</i>	<i>Polystichum munitum</i>	AM	7
<i>Populus</i>	<i>Populus X canadensis moench</i>	Ecto	1
<i>Populus</i>	<i>Populus angustifolia</i>	Ecto	21
<i>Populus</i>	<i>Populus balsamifera</i>	Ecto	93
<i>Populus</i>	<i>Populus balsamifera L.</i>	Ecto	22
<i>Populus</i>	<i>Populus balsamifera L.</i>	Ecto	6
<i>Populus</i>	<i>Populus balsamifera L. var. balsamifera</i>	Ecto	84
<i>Populus</i>	<i>Populus fremontii</i>	Ecto	3
<i>Populus</i>	<i>Populus tremuloides</i>	Ecto	7
<i>Portulaca</i>	<i>Portulaca oleracea</i>	AM	1
<i>Potentilla</i>	<i>Potentilla</i>	AM	2
<i>Potentilla</i>	<i>Potentilla crinita</i>	AM	1
<i>Potentilla</i>	<i>Potentilla hippeana</i>	AM	1
<i>Potentilla</i>	<i>Potentilla hippiana</i>	AM	1
<i>Potentilla</i>	<i>Potentilla subviscosa</i>	AM	1
<i>Prunus</i>	<i>Prunus ilicifolia</i>	AM	1
<i>Pseudocymopterus</i>	<i>Pseudocymopterus montanus</i>	AM	2
<i>Pseudognaphalium</i>	<i>Pseudognaphalium macounii</i>	AM	1
<i>Pseudotsuga</i>	<i>Pseudotsuga menziesii</i>	Ecto	23
<i>Pteridium</i>	<i>Pteridium aquilinum</i>	AM	7
<i>Quercus</i>	<i>Quercus agrifolia</i>	Ecto	1
<i>Quercus</i>	<i>Quercus douglasii</i>	Ecto	2
<i>Quercus</i>	<i>Quercus durata</i>	Ecto	1

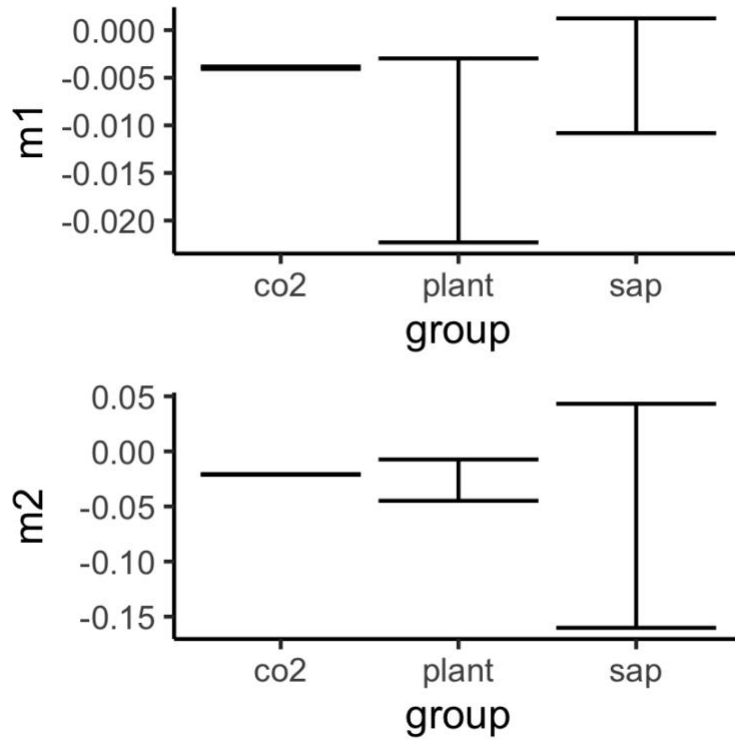
<i>Quercus</i>	<i>Quercus gambelii</i>	Ecto	1
<i>Quercus</i>	<i>Quercus lobata</i>	Ecto	1
<i>Quercus</i>	<i>Quercus rubrum</i>	Ecto	2
<i>Quercus</i>	<i>Quercus velutina</i>	Ecto	1
<i>Ranunculus</i>	<i>Ranunculus uncinatus</i>	AM	3
<i>Rhamnus</i>	<i>Rhamnus crocea</i>	AM	1
<i>Ribes</i>	<i>Ribes sanguineum</i>	AM	6
<i>Rosa</i>	<i>Rosa gymnocarpa</i>	AM	7
<i>Rosa</i>	<i>Rosa spp.</i>	AM	1
<i>Rosa</i>	<i>Rosa woodsii</i>	AM	1
<i>Rubus</i>	<i>Rubus leucodermis</i>	AM	7
<i>Rubus</i>	<i>Rubus parviflorus</i>	AM	7
<i>Rubus</i>	<i>Rubus spectabilis</i>	AM	4
<i>Rubus</i>	<i>Rubus ursinus</i>	AM	7
<i>Salix</i>	<i>Salix exigua</i>	Ecto	16
<i>Salix</i>	<i>Salix lasiolepis</i>	Ecto	1
<i>Salix</i>	<i>Salix lucida</i>	Ecto	1
<i>Salix</i>	<i>Salix phylicifolia</i>	Ecto	1
<i>Schizachyrium</i>	<i>Schizachyrium scoparium</i>	AM	1
<i>Senecio</i>	<i>Senecio actinella</i>	AM	1
<i>Senecio</i>	<i>Senecio eremophilus</i>	AM	1
<i>Sequoia</i>	<i>Sequoia sempervirens</i>	AM	6
<i>Solidago</i>	<i>Solidago nana</i>	AM	1
<i>Solidago</i>	<i>Solidago velutina</i>	AM	1
<i>Sorbus</i>	<i>Sorbus americana</i>	AM	5
<i>Sorbus</i>	<i>Sorbus sitchensis</i>	Ecto	1
<i>Spiraea</i>	<i>Spiraea betulifolia</i>	AM	9
<i>Sporobolus</i>	<i>Sporobolus interruptus</i>	AM	1
<i>Stachys</i>	<i>Stachys mexicana</i>	AM	6
<i>Stipa</i>	<i>Stipa comata</i>	AM	1
<i>Symphoricarpos</i>	<i>Symphoricarpos albus</i>	AM	13
<i>Symphoricarpos</i>	<i>Symphoricarpos mollis</i>	AM	2
<i>Symphyotrichum</i>	<i>Symphyotrichum ascendens</i>	AM	1
<i>Symphyotrichum</i>	<i>Symphyotrichum falcatum</i>	AM	1
<i>Synthyris</i>	<i>Synthyris reniformis</i>	AM	3
<i>Taraxacum</i>	<i>Taraxacum campylodes</i>	AM	1
<i>Taraxacum</i>	<i>Taraxacum officinale</i>	AM	1
<i>Thalictrum</i>	<i>Thalictrum fendleri</i>	AM	2
<i>Thuja</i>	<i>Thuja occidentalis</i>	AM	2

<i>Thuja</i>	<i>Thuja plicata</i>	AM	1
<i>Tilia</i>	<i>Tilia Americana</i>	AM	1
<i>Torilis</i>	<i>Torilis nodosa</i>	AM	1
<i>Townsendia</i>	<i>Townsendia exscapa</i>	AM	1
<i>Toxicodendron</i>	<i>Toxicodendron diversilobum</i>	AM	1
<i>Tragopogon</i>	<i>Tragopogon dubius</i>	AM	1
<i>Trientalis</i>	<i>Trientalis latifolia</i>	AM	7
<i>Trillium</i>	<i>Trillium ovatum</i>	AM	7
<i>Trisetum</i>	<i>Trisetum</i>	AM	2
<i>Tsuga</i>	<i>Tsuga canadensis</i>	Ecto	11
<i>Tsuga</i>	<i>Tsuga heterophylla</i>	Ecto	2
<i>Tsuga</i>	<i>Tsuga mertensiana</i>	Ecto	1
<i>Typha</i>	<i>Typha latifolia</i>	AM	1
<i>Ulmus</i>	<i>Ulmus pumila</i>	AM	2
<i>Umbellularia</i>	<i>Umbellularia californica</i>	AM	1
<i>Unidentified</i>	<i>Unidentified species: Annual grass</i>	AM	1
<i>Unidentified</i>	<i>Unidentified species: Bunch grass</i>	AM	1
<i>Unidentified</i>	<i>Unidentified species: Serpentine grass</i>	AM	1
<i>Unidentified</i>	<i>Unidentified species: Wetland grass</i>	AM	1
<i>Vancouveria</i>	<i>Vancouveria hexandra</i>	AM	7
<i>Verbascum</i>	<i>Verbascum thapsus</i>	AM	1
<i>Verbena</i>	<i>Verbena bracteata</i>	AM	1
<i>Viburnum</i>	<i>Viburnum alnifolium</i>	AM	1
<i>Viola</i>	<i>Viola canadensis</i>	AM	1
<i>Viola</i>	<i>Viola glabella</i>	AM	5
<i>Viola</i>	<i>Viola sempervirens</i>	AM	7
<i>Whipplea</i>	<i>Whipplea modesta</i>	AM	3
<i>Xanthisma</i>	<i>Xanthisma gracile</i>	AM	1

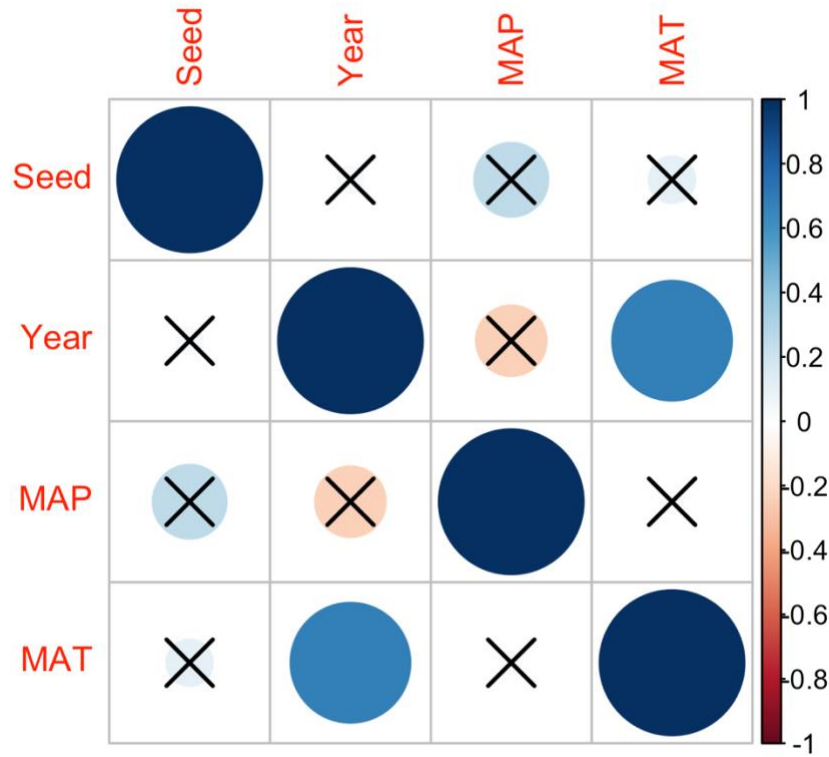
Appendix S1.5. Description of all original spatial layers included in the analysis of foliar data across the United States, with units, original resolution, source, and further details.

Data name	Data type	Original resolution	Units	Source
Soil pH x 10 in H2O 5-15 cm	soil	5000 m	pH x 10	https://www.isric.org/
Organic carbon content from 5-15 cm	soil	5000 m	dg/kg	https://www.isric.org/
Total nitrogen from 5-15 cm	soil	5000 m	cg/kg	https://www.isric.org/
Cation exchange capacity at pH 7 5-15 cm	soil	5000 m	mmol(c)/kg	https://www.isric.org/
Clay content	soil	5000 m	mass fraction ‰	https://www.isric.org/
Silt content	soil	5000 m	mass fraction ‰	https://www.isric.org/
Sand content	soil	5000 m	mass fraction ‰	https://www.isric.org/
Bulk density	soil	5000 m	cg/cm ³	https://www.isric.org/
Mean annual temperature, mean 1970-2000	climate	30 arcsec (~900m at equator)	degrees C	https://www.worldclim.org/
Mean annual precipitation, mean 1970-2000	climate	30 arcsec (~900m at equator)	mm	https://www.worldclim.org/
Aridity index	climate	1000 m	AI value	http://www.cgiar-csi.org/data/global-aridity-and-pet-database
Cultivated/managed vegetation and built environment (class 7 + 9)	biological	1000 m	percentage of land area per pixel	https://www.earthenv.org/
Woody vegetation (classes 1, 2, 3, 4, 5)	biological	1000 m	percentage of land area per pixel	https://www.earthenv.org/
Herbaceous vegetation (class 6)	biological	1000 m	percentage of land area per pixel	https://www.earthenv.org/
Arbuscular Mycorrhizal Root Stocks	biological	10000 m	Mg C ha ⁻²	https://doi.org/10.1038/s41467-019-13019-2
Ectomycorrhizal Mycorrhizal Root Stocks	biological	10000 m	Mg C ha ⁻²	https://doi.org/10.1038/s41467-019-13019-2
Net primary productivity, mean 2001-2017	climate	250 m	NPP	http://files.ntsg.umt.edu/data/NTSG_Products/MOD17/MODIS_250/modis-250-npp/

Appendix S2.1. 95% confidence intervals around the two estimates of $\delta^{13}\text{C}$ slopes over time (m1=earlier, m2=later) in atmospheric CO_2 (co2), leaves of plants (plant), and sporocarps of saprotrophic fungi (sap).



Appendix S3.1. Pairwise correlations between environmental variables. Significant correlations are shown with full circles, whereas non-significant correlations are marked with an 'X'. The sign of the correlation corresponds to the color bar on the right side. Seed = beech seed production, Year = year, MAP = mean annual precipitation. MAT = mean annual temperature.



Appendix S3.2. Identifiers, locations, and time periods of seed production datasets within the MASTREE+ data compilation that were used to calculate the index of mast seeding.

MASTREE+ identifier	study	Dataset Reference	Site Latitude	Site Longitude	Start Year	End Year
A00056		Gloaguen & Touffet 1982	48.47	-1.56	1973	1977
A00056		Gloaguen & Touffet 1982	48.47	-1.56	1970	1979
A00177		Relazioni annuali della Sezione Forestale, Canton Ticino	46.331928	8.800477	1962	1981
A00086		Jenni 1987	46.78843616	8.222420965	1905	1982
A00168		Piovesan & Bernabei 1997	42.92134816	12.1456325	1966	1994
A00036		CFS_UTB_Perri	44.297449	10.338579	1990	1995
A00036		CFS_UTB_Perri	45.838447	11.454453	1990	1996
A00036		CFS_UTB_Perri	45.900552	11.562652	1990	1996
A00036		CFS_UTB_Perri	45.785027	11.576543	1990	1996
A00036		CFS_UTB_Perri	45.940238	11.705614	1990	1996
A00036		CFS_UTB_Perri	45.620179	11.02705	1991	1996
A00036		CFS_UTB_Perri	45.862101	11.396497	1991	1996
A00166		Pilastro et al. 2003	46.07	12.38	1991	1998
A00036		CFS_UTB_Perri	45.875605	11.462777	1990	1999
A00178		Renecofor	47.79611111	5.071388889	1993	1999
A00178		Renecofor	47.79611111	5.071388889	1994	1999
A00178		Renecofor	48.64916667	6.067777778	1994	1999
A00153		Ott et al. 2003	46.78843616	8.222420965	1995	1999
A00036		CFS_UTB_Perri	45.70849	10.771317	1991	2000
A00036		CFS_UTB_Perri	45.606241	10.794812	1991	2000
A00036		CFS_UTB_Perri	45.798381	11.605639	1992	2003
A00036		CFS_UTB_Perri	45.875885	11.50962	1991	2004
A00036		CFS_UTB_Perri	45.878415	11.358135	1993	2004
A00036		CFS_UTB_Perri	45.631099	10.948535	1995	2004
A00036		CFS_UTB_Perri	45.875885	11.50962	1998	2004
A00224		Wauters et al. 2007	46.12	9.8	1999	2004
A00036		CFS_UTB_Perri	45.875885	11.50962	1999	2004
A00036		CFS_UTB_Perri	45.952943	11.017593	1990	2005
A00036		CFS_UTB_Perri	45.763026	11.153698	1990	2005
A00036		CFS_UTB_Perri	46.007737	11.412937	1990	2005
A00036		CFS_UTB_Perri	45.683335	11.216643	1992	2005
A00036		CFS_UTB_Perri	45.901611	8.826025	1993	2005

A00036	CFS_UTB_Per	45.732811	10.939889	1994	2005
A00036	CFS_UTB_Per	44.243479	8.107715	1995	2005
A00057	Granier et al. 2008	48.08333333	7.066666667	1996	2005
A00036	CFS_UTB_Per	45.787506	11.090195	1998	2005
A00036	CFS_UTB_Per	45.748346	10.242943	1999	2005
A00036	CFS_UTB_Per	46.014638	10.796939	2001	2005
A00036	CFS_UTB_Per	45.706576	10.849303	1990	2006
A00036	CFS_UTB_Per	46.142383	12.216493	1990	2006
A00036	CFS_UTB_Per	44.477177	10.085523	1993	2006
A00036	CFS_UTB_Per	46.074779	11.121749	1990	2007
A00036	CFS_UTB_Per	45.631155	10.72408	1991	2007
A00178	Renecofor	49.32416667	2.876111111	1993	2007
A00178	Renecofor	49.17083333	5.004722222	1993	2007
A00178	Renecofor	49.1825	-0.85638889	1994	2007
A00178	Renecofor	47.83777778	-3.54277778	1995	2007
A00036	CFS_UTB_Per	46.128354	12.419748	1995	2007
A00165	Pidek et al. 2010	47.344432	7.143303	1998	2007
A00036	CFS_UTB_Per	44.229992	7.665791	2003	2007
A00178	Renecofor	49.71083333	1.326111111	1993	2008
A00178	Renecofor	46.19361111	2.998333333	1993	2008
A00178	Renecofor	49.20583333	3.126666667	1993	2008
A00178	Renecofor	48.10583333	6.247222222	1993	2008
A00178	Renecofor	43.02666667	0.436666667	1994	2008
A00178	Renecofor	43.41055556	2.177777778	1994	2008
A00178	Renecofor	47.81388889	4.855	1994	2008
A00178	Renecofor	44.13111111	5.8	1994	2008
A00178	Renecofor	47.19194444	6.278055556	1994	2008
A00178	Renecofor	44.91777778	5.296111111	1995	2008
A00178	Renecofor	42.93138889	1.282222222	1996	2008
A00040	Cutini et al. 2009	43.63333333	11.9	1992	2009
A00075	Hoch et al. 2013	47.46666667	7.5	1999	2009
A00040	Cutini et al. 2009	43.65	11.91666667	2003	2009
A00041	Cutini et al. 2013	43.8	11.81666667	1991	2010
A00149	Nussbaumer et al. 2016	46.78843616	8.222420965	1986	2011
M00086	Oddou-Muratorio_2018	42.47	3.02	2002	2011
A00036	CFS_UTB_Per	45.24804402	8.746251705	2008	2012

A00036	CFS_UTB_Perì	45.4927975	11.58918006	2008	2012
A00131	Mezzavilla 2014	46.04	12.39	1991	2013
A00036	CFS_UTB_Perì	44.278154	7.384411	1994	2013
A00178	Renecofofor	43.15027778	-0.65805556	1994	2014
A00036	CFS_UTB_Perì	45.24804402	8.746251705	2007	2014
A00178	Renecofofor	44.11527778	3.543333333	1994	2015
A00033	Cansiglio; Regione Veneto	46.077209	12.3933	2011	2015
A00030	Burkart; Personal observation	47.4	8.4	1982	2016
D00022	Chianucci and Cutini, unpublished	43.66061879	11.920102	2003	2016
D00022	Chianucci and Cutini, unpublished	43.65005985	11.913902	1992	2020
D00022	Chianucci and Cutini, unpublished	43.64986697	11.91541755	1992	2020
D00022	Chianucci and Cutini, unpublished	43.66187075	11.92007872	2003	2020

Appendix S3.3. Relationship between beech seed production and fungal sporocarp community diversity (left) and richness (right), after accounting for the effects of mean annual precipitation and temperature (partial residuals). Green line represents mean line, bordered by shaded 95% confidence intervals.

